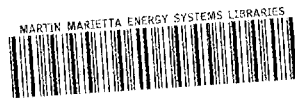


CR/RPT

ornl



3 4456 0362826 0

ORNL/TM-12183

**OAK RIDGE
NATIONAL
LABORATORY**



**Recommendations for a Kalman Filter
to Estimate and Control Freeze and
Sublime Rates of Gaseous Diffusion
Plant Freezer/Sublimers Systems**

F. R. Ruppel

OAK RIDGE NATIONAL LABORATORY
CENTRAL RESEARCH LIBRARY
CIRCULATION SECTION
ROOM ROOM 125
LIBRARY LOAN COPY
DO NOT TRANSFER TO ANOTHER PERSON
If you wish someone else to see this
report, send in name with report and
the library will arrange a loan.
RCN7984(3-77)

MANAGED BY
MARTIN MARIETTA ENERGY SYSTEMS, INC.
FOR THE UNITED STATES
DEPARTMENT OF ENERGY

This report has been reproduced directly from the best available copy.

Available to DCE and DCE contractors from the Office of Scientific and Technical Information, P.O. Box 92, Oak Ridge, TN 37831; prices available from (615) 576-8401, FTS 626-8401.

Available to the public from the National Technical Information Service, U.S. Department of Commerce, 5285 Port Royal Rd., Springfield, VA 22161.

NTIS price codes—Printed Copy: A03 Microfiche A01

This report was prepared as an account of work sponsored by an agency of the United States Government. Neither the United States Government nor any agency thereof, nor any of their employees, makes any warranty, express or implied, or assumes any legal liability or responsibility for the accuracy, completeness, or usefulness of any information, apparatus, product, or process disclosed, or represents that its use would not infringe privately owned rights. Reference herein to any specific commercial product, process, or service by trade name, trademark, manufacturer, or otherwise, does not necessarily constitute or imply its endorsement, recommendation, or favoring by the United States Government or any agency thereof. The views and opinions of authors expressed herein do not necessarily state or reflect those of the United States Government or any agency thereof.

Instrumentation and Controls Division

**RECOMMENDATIONS FOR A KALMAN FILTER TO ESTIMATE AND CONTROL
FREEZE AND SUBLIME RATES OF GASEOUS DIFFUSION PLANT
FREEZER/SUBLIMER SYSTEMS**

F. R. Ruppel

Date Published—September 1992

Prepared by
OAK RIDGE NATIONAL LABORATORY
Oak Ridge, Tennessee 37831-6285
managed by
MARTIN MARIETTA ENERGY SYSTEMS, INC.
for the
U.S. DEPARTMENT OF ENERGY
under contract DE-AC05-84OR21400



CONTENTS

| | |
|---|-----|
| LIST OF FIGURES | v |
| ABSTRACT | vii |
| 1. INTRODUCTION | 1 |
| 1.1 BACKGROUND | 1 |
| 1.2 INCENTIVE FOR USING KALMAN FILTER | 3 |
| 1.3 REPORT OVERVIEW | 3 |
| 2. FLOW MODEL DEVELOPMENT | 5 |
| 2.1 NEW MODEL DERIVATION | 5 |
| 2.2 CHECK FOR CHOKED FLOW | 9 |
| 2.3 DEAD TIME | 10 |
| 3. KALMAN FILTER DEVELOPMENT | 13 |
| 3.1 SYSTEM MODEL EQUATION | 13 |
| 3.2 MEASUREMENT MODEL EQUATION | 14 |
| 3.3 KALMAN FILTER EQUATIONS | 14 |
| 3.3.1 Computation of Kalman Gain | 14 |
| 3.3.2 Updating the Estimate | 15 |
| 3.3.3 Updating the Estimation Error Covariance Matrix | 16 |
| 3.3.4 Projecting the Estimate | 16 |
| 3.3.5 Projecting the Estimation Error Covariance Matrix | 16 |
| 3.4 DETERMINATION OF THE MODEL COVARIANCE MATRIX | 17 |
| 3.5 STEADY-STATE KALMAN FILTER | 17 |
| 3.6 OFF-LINE RESULTS FROM TEST DATA | 18 |
| 3.7 IMPLEMENTATION | 19 |
| 3.7.1 Personal Computer-Based Data Acquisition System | 19 |
| 3.7.2 Texas Instruments D/3 Control System | 19 |
| 4. CONTROL STRATEGY | 25 |
| 4.1 PROCESS MODEL-BASED CONTROL STRATEGY | 25 |
| 4.2 CONVENTIONAL LINEAR CONTROL STRATEGY | 28 |
| 5. CONCLUSIONS AND RECOMMENDATIONS | 29 |
| 6. REFERENCES | 31 |
| Appendix A. FREEZE AND SUBLIME DATA, WEIGHT-RATE AND WEIGHT COMPARISONS, AND KALMAN FILTER AND CONTROL ALGORITHM PSEUDOCODE | 33 |

LIST OF FIGURES

| | | |
|-----|--|----|
| 1.1 | Freezer/sublimer process with proposed Kalman filter to determine UF_6 freeze or sublime rate | 2 |
| 1.2 | Filtered derivative of weigh cell signal from prototype freezer/sublimer test 1126A | 2 |
| 2.1 | Summary of C_v data points | 7 |
| 2.2 | Valve characterization and test data | 9 |
| 2.3 | Check for choked flow at $U = 15\%$ | 11 |
| 2.4 | Check for choked flow at $U = 36\%$ | 11 |
| 3.1 | Analogy of Kalman filter to feedback controller | 13 |
| 3.2 | Comparison of raw weight-rate signal, modeled flow signal, and Kalman-filtered flow signal for test 1126A data | 18 |
| 3.3 | Block diagram of the continuous control strategy for Texas Instruments D/3 implementation | 21 |
| 3.4 | Digital device logical diagram for Texas Instruments D/3 control system implementation | 23 |
| 4.1 | Valve output characterization relative to flow set point with $P_1 = 9$ and $P_2 = 3$ | 26 |
| 4.2 | Valve output characterization relative to upstream pressure with $F_{sp} = 4$ and $P_2 = 3$ | 26 |
| 4.3 | Valve output characterization relative to downstream pressure with $F_{sp} = 4$ and $P_2 = 3$ | 27 |
| 4.4 | Schematic of nonlinear control strategy using Kalman filter | 27 |

ABSTRACT

A signal is required to control the flow of UF_6 in gaseous diffusion plant freezer/sublimator systems. The original strategy envisioned for deriving a flow signal was to take the derivative of the freezer/sublimator weigh cell signal. However, the derivative of the digitized weight signal is noisy, preventing good control. In addition, a disturbance is introduced into the weight derivative signal because a refrigerant is circulated through a shell-and-tube heat exchanger inside the freezer/sublimator. The weight of the refrigerant is included in the weight measured by the weigh cell. If the circulation rate of the refrigerant is not steady state, a disturbance exists.

Measurements of upstream pressure, vessel pressure, and output to the system control valve are available to the control system. Thus, if the flow through the control valve is characterized properly by these measurements, a Kalman filter can be used in conjunction with these auxiliary inputs and the weigh cell input to overcome the noise and disturbance problem and provide an improved estimate of flow rate.

A discussion of the development of a Kalman filter that could be used for this application is given, and recommendations are given for its implementation.

1. INTRODUCTION

The purpose of gaseous diffusion plant freezer/sublimator systems is to control the inventory of UF_6 in the process cascade. When it is desired to decrease process inventory, UF_6 vapor is transferred from the process cascade into the freezer/sublimator and frozen out. When it is desired to increase process inventory, UF_6 is sublimated out of the freezer/sublimator and transferred back to the process cascade. This process technology has proven to be economically attractive for gaseous diffusion plants because it enables the plant to increase power usage during periods of low electrical utility demands—such as at night when inexpensive, nonfirm power is available—and decrease power usage during periods of high electrical utility demands. Power usage is proportional to process inventory. Control of freeze rate and sublime rate is important to this operation, especially when several freezer/sublimator systems must operate in harmony during a major inventory swing. The purpose of this report is to recommend an improved method to estimate and control the freeze and sublime rates of freezer/sublimator systems.

1.1 BACKGROUND

To control the flow of UF_6 into the freezer/sublimator during freeze mode and out of the freezer/sublimator during sublime mode, a flow signal is required. The original strategy envisioned for deriving a flow signal was to take the derivative of the freezer/sublimator weigh cell signal. Because flow phenomena exhibit relatively fast dynamics compared with other typical process signals, measurement samples should be taken at a rate not less than once per second to ensure good controllability. Because the weigh cell has such a broad range, little resolution will exist between samples. At a sample rate of once per second, the derivative of the digitized weight signal used by the control system will be very noisy.

Another problem associated with the weight derivative method is that unobservable inputs are present in the freezer/sublimator system. As shown in Fig. 1.1, Freon-114 is used to cool and heat the freezer/sublimator system during freeze and sublime modes respectively. The weight of the Freon-114 is included in the weight measured by the weigh cell. If the circulation rate of Freon-114 is anything but steady state, an unobservable input is added to the weight-rate signal. The beginning of a typical freeze operation of the prototype freezer/sublimator system at the Paducah Gaseous Diffusion Plant (PGDP) in Paducah, Kentucky, is shown in Fig. 1.2. The filtered weight-rate signal has many oscillations. On the basis of this signal alone, it appears that a flow reversal has occurred. However, pressure measurements taken inside the vessel and upstream of the control valve do not confirm this. Obviously, the signal has been corrupted. A current hypothesis is that the period of oscillations in the graph corresponds to the time it takes for Freon-114 to make one pass through its circuit. The step change in UF_6 flow causes a perturbation in the Freon-114 circulation rate that is a function of the flow rate and circuit path length of the Freon-114.

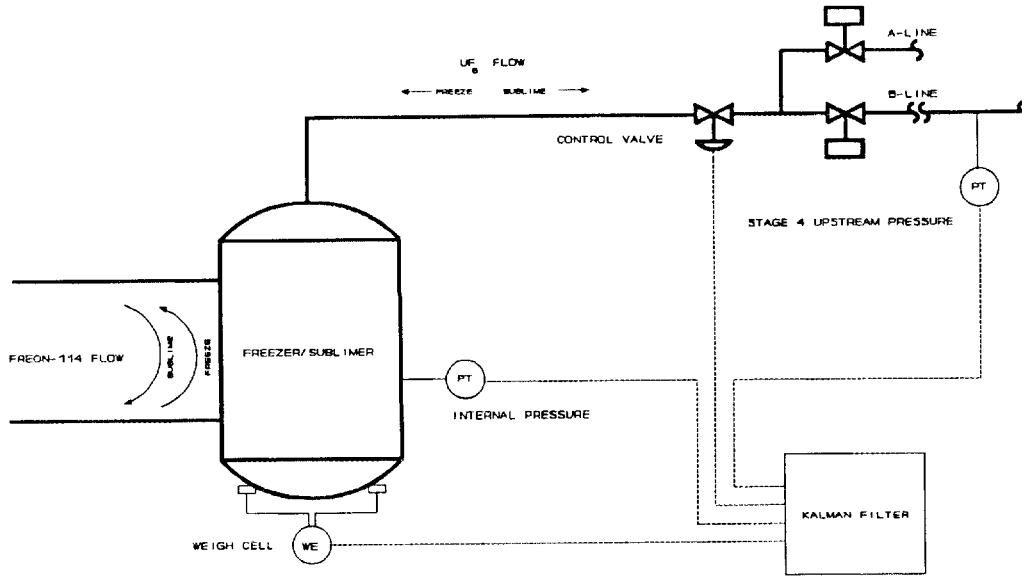


Fig. 1.1. Freezer/sublimer process with proposed Kalman filter to determine UF_0 freeze or sublime rate.

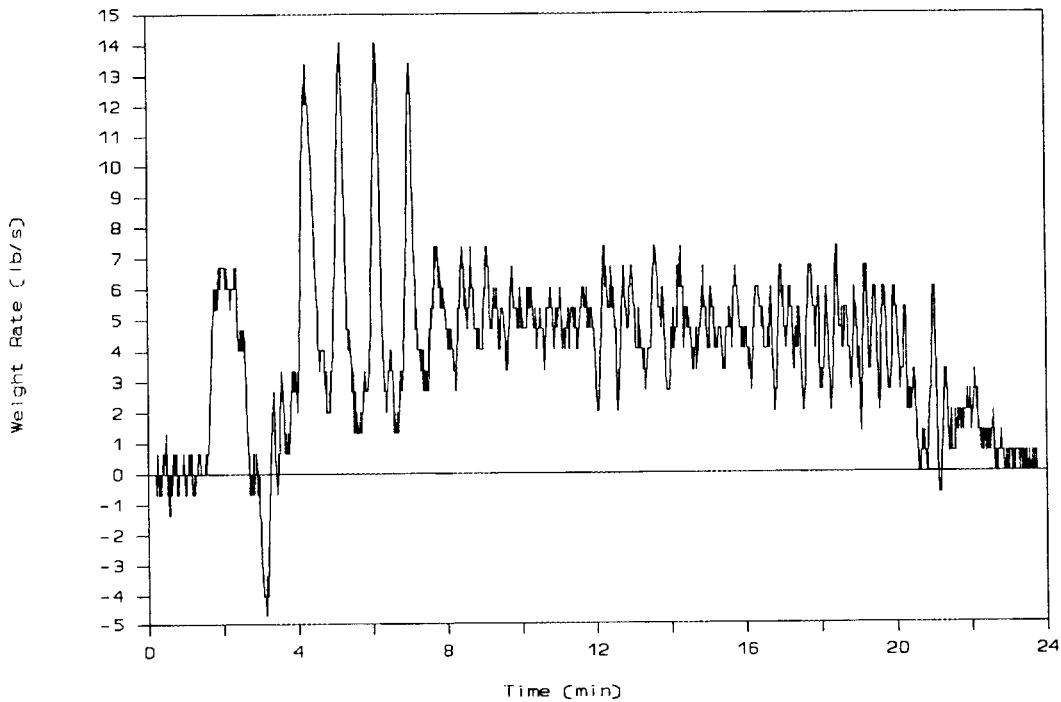


Fig. 1.2. Filtered derivative of weigh cell signal from prototype freezer/sublimer test 1126A.

1.2 INCENTIVE FOR USING KALMAN FILTER

A successful implementation of a Kalman filter has been used by Dow Chemical Company in an application very similar to ours.¹ The idea behind the method is to use other inputs in addition to the weigh cell signal to obtain the desired UF_6 flow rate. In our application, vessel pressure, stage 4 upstream pressure, and the control valve output signals are all available to facilitate the determination of flow rate. The additional measurements can be combined with a mathematical model of the system to obtain an improved status of weight rate. This approach is shown in Fig. 1.1.

1.3 REPORT OVERVIEW

The first exercise that must be undertaken is to derive the system model. This exercise is detailed in Sect. 2. Section 3 discusses the development and application of the Kalman filter to the system. A control strategy based on the Kalman filter technique is presented in Sect. 4. Section 5 summarizes the major conclusions and recommendations of this work.

2. FLOW MODEL DEVELOPMENT

To help develop a simulator/trainer system for the process inventory control system (PICS) project, a previous flow model had been developed from earlier, limited testing of the freezer/sublimator system.² This model proved unsatisfactory on the basis of new data. Therefore, a new approach was taken to improve the flow model for use with the Kalman filter.

2.1 NEW MODEL DERIVATION

Empirical data were used to develop the flow model for the freezer/sublimator system. A series of test data was taken in late 1990 to help characterize flow through the weight-rate control valve. Pertinent data consisted of freezer/sublimator internal pressure, upstream stage 4 pressure, control valve output signal, and vessel weight.

An expression that describes compressible flow through a control valve is given by³

$$F = N'' F_p C_v P_1 Y \sqrt{\frac{XM}{T_1 Z}}, \quad (2.1)$$

where

$$X = \frac{P_1 - P_2}{P_1}, \quad (2.2)$$

and

F = flow rate,

N'' = numerical constant,

F_p = piping geometry factor,

C_v = valve flow coefficient,

P_1 = upstream absolute pressure,

P_2 = downstream absolute pressure,

Y = gas expansion factor,

X = ratio of pressure drop across valve to absolute upstream pressure,

M = molecular weight of fluid,

T_1 = upstream absolute temperature,

Z = gas compressibility factor.

In the data gathered at Paducah on the prototype freezer/sublimator, the upstream temperature was not measured and will have to be considered a constant. The terms N'' , F_p , M , and Z are also constant. Combining constants in Eq. (2.1) yields

$$F = N'YP_1C_v\sqrt{X} , \quad (2.3)$$

where N' is a proportionality constant. The gas expansion factor varies from 1 (when $X = 0$) to 0.67 (when flow is choked). Also at choked flow, X has an upper limit. The valve flow coefficient C_v is predominantly a function of the valve position u . In the earlier flow model development, it was attempted to characterize the system on the basis of a single freezer/sublimator run in which valve position changed constantly. C_v , N' , and the point of choking were all determined from a single set of data. Because more data were available for the second model development, a new approach was taken in which the system characteristics were based on several runs of the system. In addition, the new data contained periods where the control valve position remained constant for long periods, thus allowing a better characterization at that valve position. In the earlier model development, three C_v relationships were assumed, and the best was chosen on the basis of least-squares analysis. The new model development consists of taking data at several valve positions and determining the C_v function from this, rather than assuming a relationship. To find the relationship, Eq. (2.3) is solved for C_v , or $F/(N'YP_1\sqrt{X})$. Valve choking and the gas expansion factor are addressed in Sect. 2.2. For now, assume $Y = 1$.

The method consisted of plotting data points of $F/(P_1\sqrt{X})$ vs u , where F is found by using the weight derivative during periods when the Freon-114 circulation rate was considered to be at steady state. The plot is shown in Fig. 2.1 for different data sets. The next step was to find an equation that provides the best fit of the data. Roffel and Rijnsdorp describe a valve characterization of the following form which appears to match our data,⁴

$$C_v = \frac{N}{\sqrt{1 + \alpha R_v^{2(1-u)}}} , \quad (2.4)$$

where N is a constant that we will use to incorporate the proportionality constant of Eq. (2.3) with that required for the C_v relationship here, α is the ratio of the squares of system capacity to valve capacity, R_v is the valve rangeability, and u is the valve output scaled between 0 and 1. It is necessary to solve Eq. (2.4) for the three parameters N , α , and R_v by using data from tests. Because the equation is nonlinear, a least-squares solution cannot be solved explicitly. However, preliminary parameters can be found by a method in which a computer program is written to scan through bracketed values of each parameter by using nested loops and saving the set of parameters with the least sum of squared errors compared to the test data. The values of the parameters are bracketed by using engineering judgment. The interval between the bracketed values is divided into as many subintervals as is practical. A computer program uses nested loops to loop through each value of each parameter, and the sum of squared errors as compared with actual data is computed. As the program proceeds from loop to loop, the least sum of squared errors is saved along with the values of the parameters for the least sum. A preliminary set of parameters ($N = 1.6$, $\alpha = 0.029$, and $R_v = 47$) was derived by using this method. However, this method does not provide the optimum solution, because it depends on the

resolution assigned to the parameters in the bracketed method (i.e., the number of subintervals that the bracketed values are divided into).

A better method can be used that begins with the preliminary parameters and uses a linearized sum of squares to provide a better fit to the data. A truncated Taylor series expansion is performed on Eq. (2.4). Partial derivatives are required for the truncated Taylor series expansion. Partial derivatives of Eq. (2.4) with respect to the three parameters are given in the next three equations.

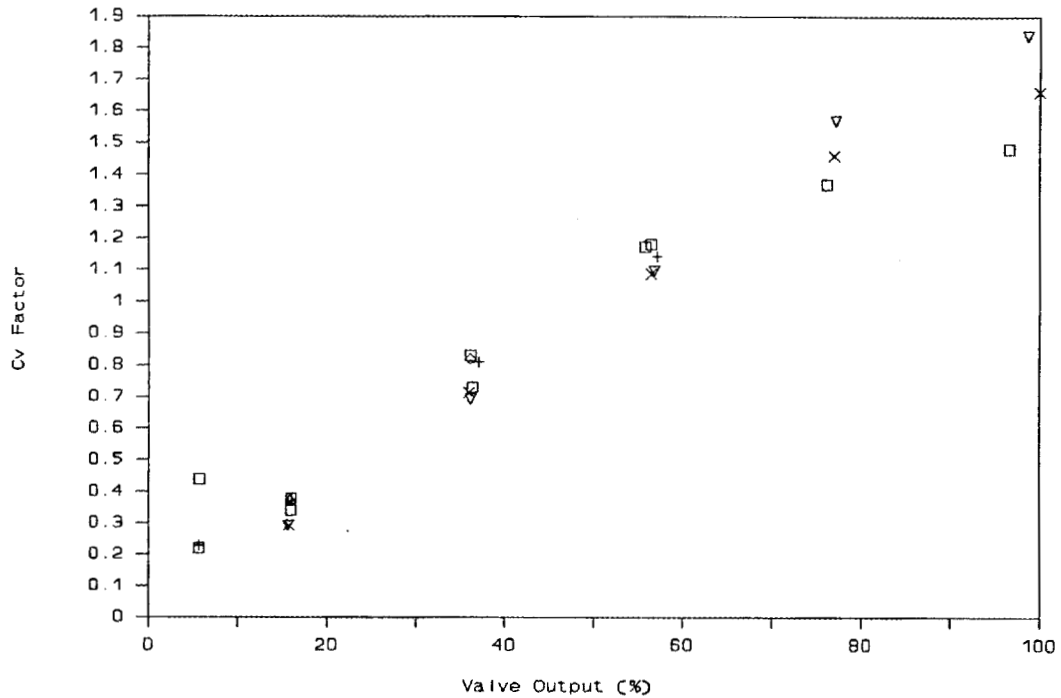


Fig. 2.1. Summary of C_v data points. Symbols refer to test numbers: \square , 1106C; $+$, 1103C; \diamond , 1126A; Δ , 1110A; \times , 1108B; and ∇ , 1103E.

$$\frac{\partial C_v}{\partial N} = \frac{1}{\sqrt{1 + \alpha R_v^{2(1-n)}}} \quad (2.5)$$

$$\frac{\partial C_v}{\partial \alpha} = -\frac{1}{2} N [1 + \alpha R_v^{2(1-n)}]^{-\frac{3}{2}} R_v^{2(1-n)} \quad (2.6)$$

$$\frac{\partial C_v}{\partial R_v} = -\alpha N(1-u)R_v^{(1-2u)} \left[1 + \alpha R_v^{2(1-u)} \right]^{\frac{3}{2}} . \quad (2.7)$$

The truncated Taylor series expansion, using only first partial derivatives, is given by the following equation, where the deltas refer to changes in parameters from their initial values, and the zero subscripts refer to the initial parameter values, which is where the partial derivatives are evaluated:

$$\frac{F}{P_1\sqrt{X}} = C_v(u, N_0, \alpha_0, R_{v_0}) + \frac{\partial C_v}{\partial N} \Delta N + \frac{\partial C_v}{\partial \alpha} \Delta \alpha + \frac{\partial C_v}{\partial R_v} \Delta R_v . \quad (2.8)$$

Because Eq. (2.8) is linear, it can be solved by traditional least-squares techniques. All variables in Eq. (2.8), except parameter-related values, can be obtained from experimental testing. Described earlier was how to derive initial values of the parameters; changes from those initial values, ΔN , $\Delta \alpha$, and ΔR_v , are what we are solving for. With several sets of data, a matrix is set up of the following form, where the nonzero subscripts refer to data point numbers:

$$\begin{bmatrix} \frac{F_1}{P_{1_1}\sqrt{X_1}} - C_v(u_1, N_0, \alpha_0, R_{v_0}) \\ \frac{F_2}{P_{1_2}\sqrt{X_2}} - C_v(u_2, N_0, \alpha_0, R_{v_0}) \\ \cdot \\ \cdot \\ \cdot \\ \frac{F_n}{P_{1_n}\sqrt{X_n}} - C_v(u_n, N_0, \alpha_0, R_{v_0}) \end{bmatrix} = \begin{bmatrix} \frac{\partial C_v(u_1)}{\partial N} & \frac{\partial C_v(u_1)}{\partial \alpha} & \frac{\partial C_v(u_1)}{\partial R_v} \\ \frac{\partial C_v(u_2)}{\partial N} & \frac{\partial C_v(u_2)}{\partial \alpha} & \frac{\partial C_v(u_2)}{\partial R_v} \\ \cdot & \cdot & \cdot \\ \cdot & \cdot & \cdot \\ \cdot & \cdot & \cdot \\ \frac{\partial C_v(u_n)}{\partial N} & \frac{\partial C_v(u_n)}{\partial \alpha} & \frac{\partial C_v(u_n)}{\partial R_v} \end{bmatrix} \begin{bmatrix} \Delta N \\ \Delta \alpha \\ \Delta R_v \end{bmatrix} , \quad (2.9)$$

or

$$y = \Phi \theta , \quad (2.10)$$

where y is an $(n \times 1)$ vector, Φ is an $(n \times 3)$ matrix, and θ is a (3×1) vector. This matrix equation is over-specified when the number of data points exceeds the number of parameters being solved for as is our case. The equation is solved by using the least-squares technique with

$$\theta = (\Phi^T \Phi)^{-1} \Phi^T y . \quad (2.11)$$

Equation (2.11) is solved, the changes are made to the parameters, the parameters are reentered into the equation as new initial values, and the routine is continued iteration by iteration until the parameters change no more than a specified tolerance. The parameters, as determined by this exercise, are $N = 1.69$, $\alpha = 0.055$, and $R_v = 33.7$. The fit is shown in Fig. 2.2. Because a butterfly valve is used as the system control valve, leakage exists when the valve is closed. That is why the curve does not go through the origin.

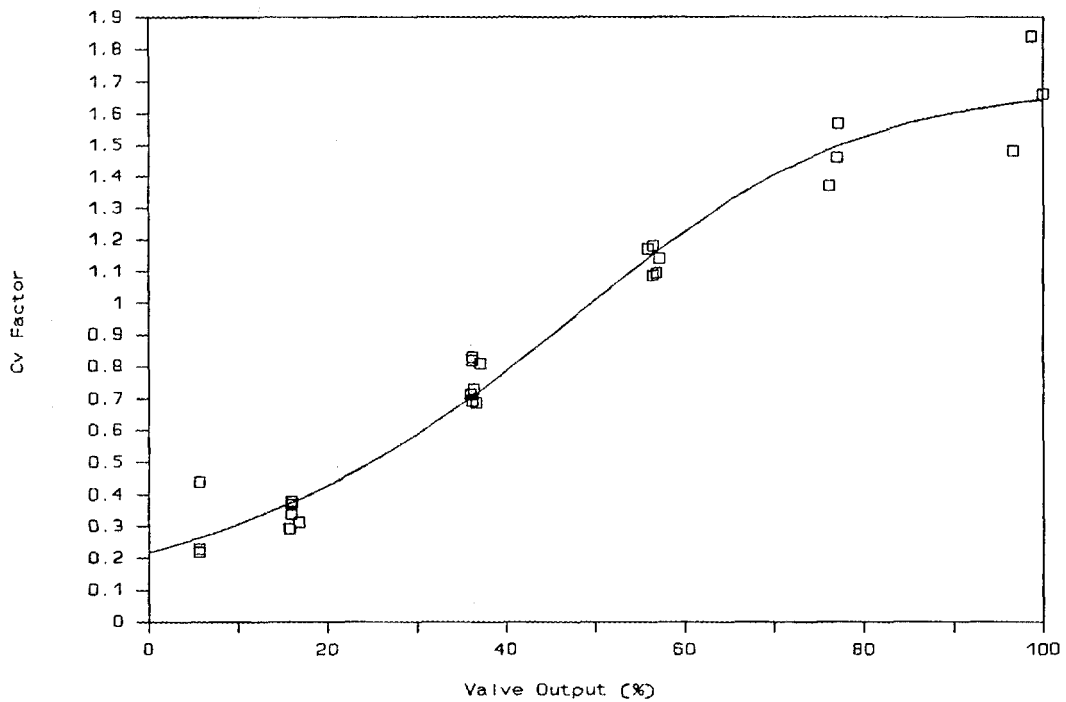


Fig. 2.2. Valve characterization and test data.

2.2 CHECK FOR CHOKED FLOW

Choked flow exists when flow is no longer a function of \sqrt{X} , usually occurring when downstream pressure drops to the point where flow is sonic through the *vena contracta* of a control valve. Further decreases in downstream pressure do not result in further increases in flow rate—sonic flow is the limiting factor. To check for choked flow, a graph of F/P_1 vs \sqrt{X} was prepared at constant valve positions u . If flow choking exists in the flow regime of interest, F/P_1 will be a linear function of \sqrt{X} until a maximum \sqrt{X} is reached. At this point, F/P_1 will level off and will no longer be a function of \sqrt{X} . Two

examples are shown using data from the tests at Paducah. Enough data to make this test are available at only two valve positions, at ~15% and ~36%. Figure 2.3 shows the test at ~15%, and Fig. 2.4 shows the test at ~36%. In each figure, two clusters of data are present: a set at lower \sqrt{X} and a set at somewhat higher \sqrt{X} . If F/P_1 is strictly linear with \sqrt{X} , a straight line should go through both sets of data and the origin. If choking exists, a line through the origin and the lower set of data may not go through the higher set of data. The data in Fig. 2.3 show a strong argument that choked flow exists at $\sqrt{X} = 0.71$ or $X = 0.50$. However, Fig. 2.4 is not such a strong argument. If there is choking, it exists around $\sqrt{X} = 0.81$ or $X = 0.66$. In both cases, the determination of the C_v function will not worsen considerably if it is assumed that choked flow is not present. Notice also that the gas expansion factor is assumed to be unity. Because this value is a function of flow choking, it is difficult to specify the gas expansion factor without more knowledge of choking conditions. Attempts to incorporate the gas expansion factor scattered the data more than the data shown in Fig. 2.2. Given the fact that this model will be used as only a starting point estimate in the Kalman filter, it is not worthwhile to determine a flow equation with any more accuracy than shown here. The modeled flow will be compared with on-line data to determine a refined estimate.

The resulting model of flow (or weight rate) as a function of upstream stage 4 pressure, vessel pressure, and valve position is shown in the next equation. In freeze mode, P_1 is upstream stage 4 pressure and P_2 is the vessel pressure. In sublime mode, P_1 is the vessel pressure and P_2 is upstream stage 4 pressure divided by 5. Based on operating experience, the rule of thumb is that A-line pressure is about one fifth B-line pressure. During freeze mode, UF_6 is transferred from B-line; and in sublime mode, UF_6 is transferred to A-line:

$$F = \frac{NP_1\sqrt{X}}{\sqrt{1 + \alpha R_v^{2(1-u)}}} . \quad (2.12)$$

2.3 DEAD TIME

Because the control valve is not in very close proximity to the freezer/sublimator vessel, a dead time will exist between the time action is taken at the control valve and the time a corresponding change is noticed in the reading from the weigh cell. Tests have shown that this dead time is on the order of 10 to 12 s. Therefore, in calculations where the weight rate, as determined from weigh cell readings, is compared with the flow rate, as determined from the model developed here, dead time τ_d should be included in the equation as shown in

$$\frac{\Delta W}{\Delta t} = F(k - \tau_d) = \frac{NP_1(k - \tau_d)\sqrt{X(k - \tau_d)}}{\sqrt{1 + \alpha R_v^{2[1-u(k-\tau_d)]}}} . \quad (2.13)$$

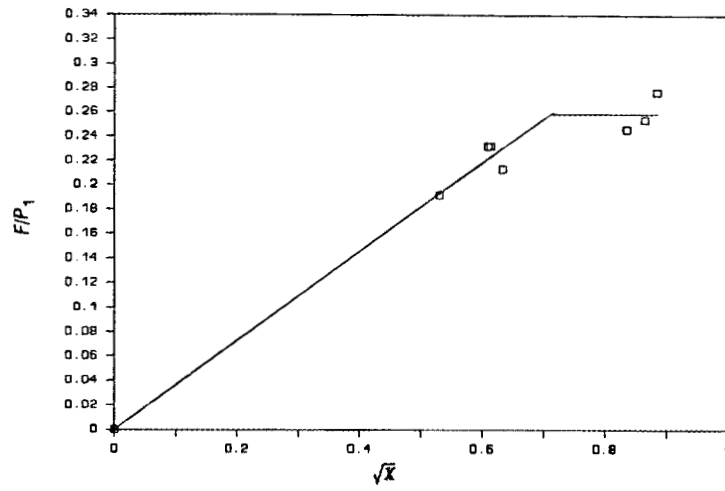


Fig. 2.3. Check for choked flow at $U \sim 15\%$.

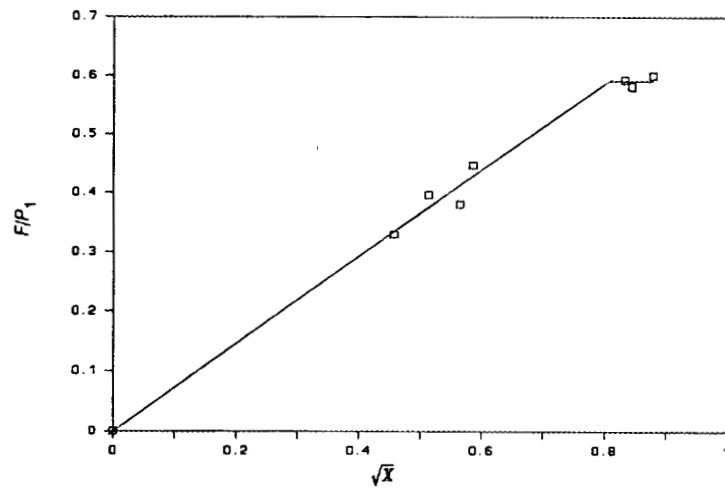


Fig. 2.4. Check for choked flow at $U \sim 36\%$.

3. KALMAN FILTER DEVELOPMENT

A Kalman filter is analogous to closed-loop control in that it samples a measurement, compares this measurement against its own estimate, and takes corrective action via the Kalman gain and the error between the two. A schematic is shown in Fig. 3.1. A full-fledged Kalman filter recursively adjusts the Kalman gain K to minimize the covariance matrix of the error between the actual measurement and the estimate. Steady-state Kalman filters use a constant value for the Kalman gain that has been derived by analysis of filter performance. Development of the flow model for our system was covered in Sect. 2. This model will be used by the Kalman filter. Development of a full-fledged Kalman filter as well as a steady-state filter for freezer/sublimer systems is presented in this section. In our system, the plant and model observable inputs are the control valve signal, upstream pressure, and downstream pressure. The unobservable input is Freon-114 weight. The measurement is freezer/sublimer weight, and the estimates are flow and freezer/sublimer weight.

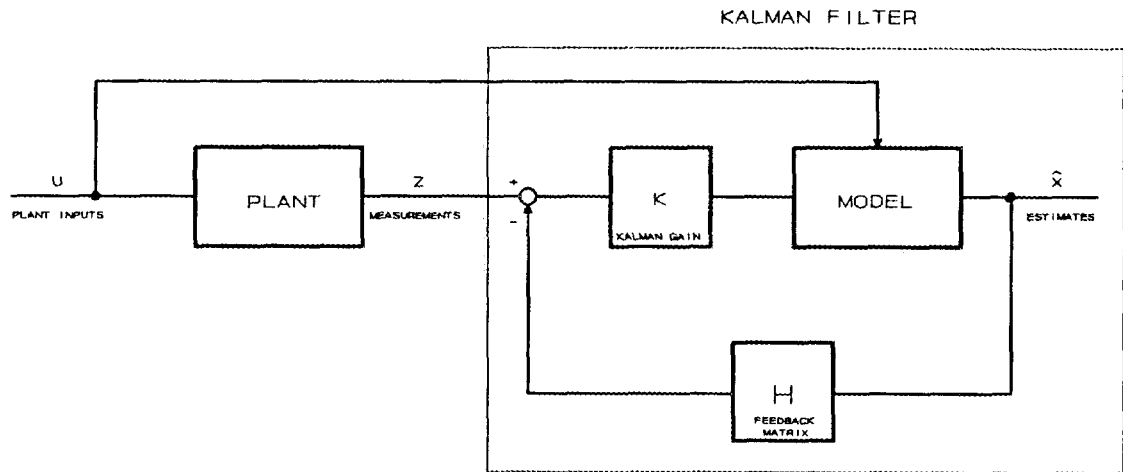


Fig. 3.1. Analogy of Kalman filter to feedback controller.

3.1 SYSTEM MODEL EQUATION

The system model equation is represented in state space discrete-time form by the following general matrix equation, where A is the state matrix, B is the input matrix, x is the state vector u is the input vector (not to be confused with the scalar u used as valve position in the preceding section), and w is noise, or the mismatch between the model and actual data:

$$x(k+1) = Ax(k) + Bu(k) + w(k) . \quad (3.1)$$

For our system, we are interested in two states: flow (or weight rate) and weight. The inputs to the system are upstream and downstream pressure and control valve output. Because the relationship of these inputs to actual flow and weight is nonlinear, it is easier to use modeled flow as the input. The linearized system state equation then takes the following form, where x_1 = flow or weight rate, x_2 = weight, and F = modeled flow:

$$\begin{bmatrix} x_1(k+1) \\ x_2(k+1) \end{bmatrix} = \begin{bmatrix} 1 & 0 \\ \Delta t & 1 \end{bmatrix} \begin{bmatrix} x_1(k) \\ x_2(k) \end{bmatrix} + \begin{bmatrix} 1 \\ 0 \end{bmatrix} [F(k+1) - F(k)] + \begin{bmatrix} w_1(k) \\ w_2(k) \end{bmatrix}. \quad (3.2)$$

3.2 MEASUREMENT MODEL EQUATION

The state space measurement equation, in general, is given by the following matrix equation:

$$z(k) = Hx(k) + v(k), \quad (3.3)$$

where z is the measurement vector, H is the measurement matrix, and v is the measurement noise. For our system, weight is the only real measurement—other inputs are incorporated into the model. The equation is

$$z(k) = [0 \ 1] \begin{bmatrix} x_1(k) \\ x_2(k) \end{bmatrix} + v(k). \quad (3.4)$$

3.3 KALMAN FILTER EQUATIONS

A classical Kalman filter consists of five distinct steps^{5,6}: (1) computation of Kalman gain, (2) updating the estimate, (3) updating the covariance matrix, (4) projecting the estimate, and (5) projecting the covariance matrix. The classical equations and corresponding equations for our application are shown in this section.

3.3.1 Computation of Kalman Gain

Computation of the Kalman gain is given by the following matrix equation:

$$K(k) = P(k)H^T [HP(k)H^T + R(k)]^{-1}, \quad (3.5)$$

where K is the Kalman gain, P is the estimation error covariance matrix, and R is the covariance matrix of the measurement noise v . Because there is only one measurement (weight), R is a scalar and can be represented by r , the variance of the weight measurement. The remainder of the equation is broken down as follows, where p_{ij} are elements of the estimation error covariance matrix: Then the Kalman gain equation for our system is

$$\begin{aligned}
\mathbf{HPH}^T &= [0 \ 1] \begin{bmatrix} p_{11} & p_{12} \\ p_{21} & p_{22} \end{bmatrix} \begin{bmatrix} 0 \\ 1 \end{bmatrix} \\
&= [0 \ 1] \begin{bmatrix} p_{11} \\ p_{22} \end{bmatrix} \\
&= p_{22} ,
\end{aligned} \tag{3.6}$$

$$\mathbf{PH}^T = \begin{bmatrix} p_{11} & p_{12} \\ p_{21} & p_{22} \end{bmatrix} \begin{bmatrix} 0 \\ 1 \end{bmatrix} = \begin{bmatrix} p_{12} \\ p_{22} \end{bmatrix} . \tag{3.7}$$

$$\mathbf{K}(k) = \begin{bmatrix} p_{12} \\ p_{22} \end{bmatrix} \frac{1}{p_{22} + r} = \begin{bmatrix} \frac{p_{12}}{p_{22} + r} \\ \frac{p_{22}}{p_{22} + r} \end{bmatrix} = \begin{bmatrix} K_1(k) \\ K_2(k) \end{bmatrix} . \tag{3.8}$$

3.3.2 Updating the Estimate

The general matrix equation for updating the estimate is

$$\hat{\mathbf{x}}(k) = \hat{\mathbf{x}}^-(k) + \mathbf{K}(k)[z(k) - \mathbf{H}\hat{\mathbf{x}}^-(k)] , \tag{3.9}$$

where the hat represents an estimate and the superposed minus sign represents a preliminary estimate based on the last output projected forward one step by the system model. Then, for our system,

$$\begin{bmatrix} \hat{x}_1(k) \\ \hat{x}_2(k) \end{bmatrix} = \begin{bmatrix} \hat{x}_1^-(k) \\ \hat{x}_2^-(k) \end{bmatrix} + \begin{bmatrix} K_1 \\ K_2 \end{bmatrix} [z(k) - \hat{x}_2^-(k)] . \tag{3.10}$$

Inspection of Eq. (3.10) shows that both flow (x_1) and weight (x_2) are based on just one raw measurement, weight. This may appear odd at first, but because the units of K_1 are inverse time, then it is obvious that units of flow, or weight per unit time, are used. Equation (3.10) also points out the job of the Kalman filter—to compromise between raw measurement data and modeled data. It is easier to see this with the weight estimate. If $K_2 = 0$, the Kalman estimate is based wholly on the system model. If $K_2 = 1$, the Kalman estimate is based wholly on the raw weight measurement. In practice, the Kalman gain will lie between these two extremes.

3.3.3 Updating the Estimation Error Covariance Matrix

The general equation for updating the estimation error covariance matrix and its interpretation to our system is given by

$$\begin{aligned}
 P(k) &= [I - K(k)H] P^-(k) \\
 &= \left\{ \begin{bmatrix} 1 & 0 \\ 0 & 1 \end{bmatrix} - \begin{bmatrix} K_1 \\ K_2 \end{bmatrix} \begin{bmatrix} 0 & 1 \end{bmatrix} \right\} P^-(k) \\
 &= \begin{bmatrix} 1 & -K_1 \\ 0 & 1 - K_2 \end{bmatrix} \begin{bmatrix} p_{11} & p_{12} \\ p_{21} & p_{22} \end{bmatrix} \\
 &= \begin{bmatrix} p_{11} - K_1 p_{21} & p_{12} - K_1 p_{22} \\ p_{21} - K_2 p_{21} & p_{22} - K_2 p_{22} \end{bmatrix}.
 \end{aligned} \tag{3.11}$$

3.3.4 Projecting the Estimate

The estimate for the upcoming time step, based on the system model, equation (3.2) is

$$\begin{bmatrix} \hat{x}_1^-(k+1) \\ \hat{x}_2^-(k+1) \end{bmatrix} = \begin{bmatrix} 1 & 0 \\ \Delta t & 1 \end{bmatrix} \begin{bmatrix} \hat{x}_1(k) \\ \hat{x}_2(k) \end{bmatrix} + \begin{bmatrix} 1 \\ 0 \end{bmatrix} [F(k+1) - F(k)]. \tag{3.12}$$

3.3.5 Projecting the Estimation Error Covariance Matrix

The projection of the estimation error covariance matrix for the upcoming time step is derived as follows, where Q is the model covariance matrix:

$$\begin{aligned}
 P^-(k+1) &= AP(k)A^T + Q \\
 &= \begin{bmatrix} 1 & 0 \\ \Delta t & 1 \end{bmatrix} \begin{bmatrix} p_{11} & p_{12} \\ p_{21} & p_{22} \end{bmatrix} \begin{bmatrix} 1 & \Delta t \\ 0 & 1 \end{bmatrix} + Q \\
 &= \begin{bmatrix} p_{11} & p_{12} \\ \Delta t p_{11} + p_{21} & \Delta t p_{12} + p_{22} \end{bmatrix} \begin{bmatrix} 1 & \Delta t \\ 0 & 1 \end{bmatrix} + Q \\
 &= \begin{bmatrix} p_{11} & \Delta t p_{11} + p_{12} \\ \Delta t p_{11} + p_{21} & \Delta t^2 p_{11} + \Delta t(p_{21} + p_{12}) + p_{22} \end{bmatrix} + \begin{bmatrix} q_{11} & q_{12} \\ q_{21} & q_{22} \end{bmatrix} \\
 &= \begin{bmatrix} p_{11} + q_{11} & \Delta t p_{11} + p_{12} + q_{12} \\ \Delta t p_{11} + p_{21} + q_{21} & \Delta t^2 p_{11} + \Delta t(p_{21} + p_{12}) + p_{22} + q_{22} \end{bmatrix}.
 \end{aligned} \tag{3.13}$$

3.4 DETERMINATION OF THE MODEL COVARIANCE MATRIX

The model covariance matrix Q is a measure of the model vs data mismatch shown by w in Eq. (3.1). It can be determined from experimental data. The definition of the covariance matrix is given in the following equation, where x is the state vector that contains both the flow state and the weight state, and the tilde refers to modeled values of the state vector based on the system model equation (3.2):

$$Q = E\{(x - \tilde{x})(x - \tilde{x})^T\}. \quad (3.14)$$

For our system, the model covariance is a (2×2) matrix of the form

$$Q = \begin{bmatrix} E\{(x_1 - \tilde{x}_1)^2\} & E\{(x_1 - \tilde{x}_1)(x_2 - \tilde{x}_2)\} \\ E\{(x_2 - \tilde{x}_2)(x_1 - \tilde{x}_1)\} & E\{(x_2 - \tilde{x}_2)^2\} \end{bmatrix}. \quad (3.15)$$

Notice that to determine Q properly, a value of x_1 flow is needed. Because an actual measurement of flow is not available, the derivative of weight was used. Because the correlation of UF_6 flow rate to the weight derivative varies from data set to data set (it is affected by Freon-114 flow rate), several of the data sets must be analyzed to yield a general value for the model covariance. This was done by determining the model covariance matrix of all the data sets shown in Appendix A and choosing the model covariance matrix whose element values lay in the midrange of all element values of the complete set of data. The matrix chosen is

$$Q = \begin{bmatrix} 0.13 & 7.2 \\ 7.2 & 2900 \end{bmatrix}. \quad (3.16)$$

Values of the elements of the covariance matrix affect how the Kalman filter will compromise between the system model and the raw measurements. As the ratio q_{11}/q_{22} increases, x_1 will follow measurements closer; when the ratio decreases, x_1 will follow the model closer.

3.5 STEADY-STATE KALMAN FILTER

The estimation error covariance matrix element values usually will converge to a constant over a certain length of time. A simplified, steady-state Kalman filter can be used that is based on the ultimate values of the covariance values. Tests of the prototype data show that values converge to $K_1 = 0.0067$ and $K_2 = 0.995$ given the covariances in Eq. (3.16). The closeness of the value of K_2 to one indicates that an estimate of weight is probably not necessary; the raw value could be used just as well.

3.6 OFF-LINE RESULTS FROM TEST DATA

A comparison of the original filtered weight-rate signal, modeled flow signal, and Kalman-filtered flow signal for Test 1126A is shown in Fig. 3.2. The original data are the same as those shown in Fig. 1.2. As described earlier, the original weight-rate signal shows extreme oscillations, so extreme that flow reversal is implied. The modeled flow does show high initial flow followed by one valley before stabilizing. However, an offset exists between the modeled flow and the raw weight-rate signal after the raw signal has stabilized. The Kalman-filtered signal begins with a high initial signal followed by a valley lower than that of the modeled signal, but the Kalman-filtered signal then converges with the raw weight-rate signal after the raw signal has stabilized.

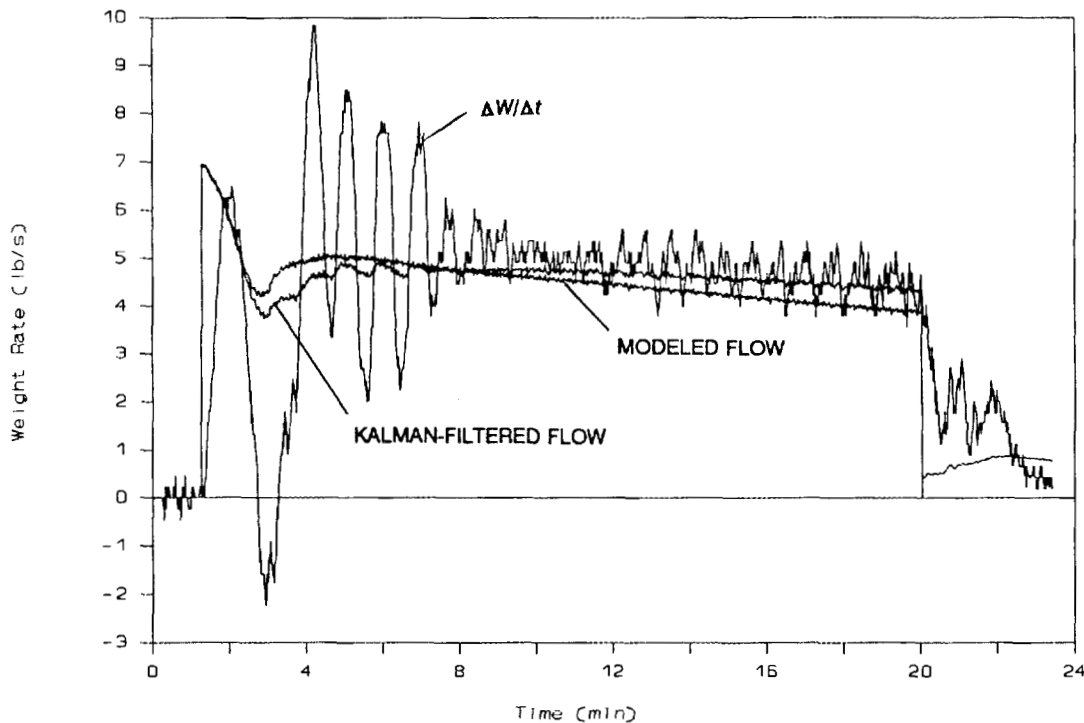


Fig. 3.2. Comparison of raw weight-rate signal, modeled flow signal, and Kalman-filtered flow signal for test 1126A data.

Plots of all the experimental data sets are compared in Appendix A. In addition to the weight-rate comparisons, graphs of weight comparisons between the actual vessel weight and the weight as determined by integrating the Kalman-estimated flow are shown. The vessel weight signal is less noisy than the raw weight rate signal; therefore, it serves as a better guide as to whether the Kalman-estimated flow signal is accurate. The two signals should converge. In the graphs of sublime tests, the integrated Kalman flow signal is reset to that of the raw weight signal after completion of the Freon-114 transfers. The Freon-114 transfer in sublime mode represents a drastic bias error to the weight derivative and, consequently, an error in the flow signal. Therefore, at the beginning of sublime mode (for the first ~220 s) the Kalman filter should be coded to rely totally on the

modeled flow rate and to ignore the weight signal. The sublime-mode graphs in Appendix A reflect the addition of this code to the Kalman filter.

Given the results of the test data, it appears that a Kalman filter is useful in this application. However, on-line testing of the Kalman filter should be carried out before proceeding fully. Because more instrumentation is involved in deriving the weight-rate signal using this method, calibration of one instrument with respect to another becomes more crucial. Preliminary testing data indicate that at low flow rates, zero shifts in the pressure transmitters may cause a problem not only because of a negative differential pressure but also because the square root of this signal is taken. A square root taken of a negative signal would cause an error in the processing algorithm.

3.7 IMPLEMENTATION

The analysis up to this point may seem to indicate that the Kalman filter is a complicated system. Like many developments, the theory behind the implementation is more complicated than the actual mechanism for carrying out the implementation. In our case, the Kalman filter can be coded into standard data acquisition and control systems.

3.7.1 Personal-Computer-Based Data Acquisition System

A pseudolisting of code is given in Appendix A which can be used to test the Kalman filter on the prototype freezer/sublimator system by using a personal-computer-based data acquisition system. This listing is for the steady-state Kalman filter; the full-fledged Kalman filter would take more code than shown here.

3.7.2 Texas Instruments D/3 Control System

Figures 3.3 and 3.4 represent an implementation of the Kalman filter in the Texas Instruments D/3 control system. Figure 3.3 is a block diagram of the continuous control strategy required, and Fig. 3.4 is a logic diagram of a device that feeds status bits to the continuous control strategy. The D/3 is the control system chosen for inventory control at PGDP. The Kalman filter is not a straightforward application for the fill-in-the-blank, connect-the-block configuration used in control systems like the D/3. However, the strategy is implementable, and if greater processing capability is required, the D/3 Sequencing and Batch Language could be used. The digital device logic assumes that signals are available to determine whether the system is in freeze or sublime mode. The diagrams shown here convey the concept for implementation. The actual configuration will probably differ when the strategy is studied in detail by the end programmer.

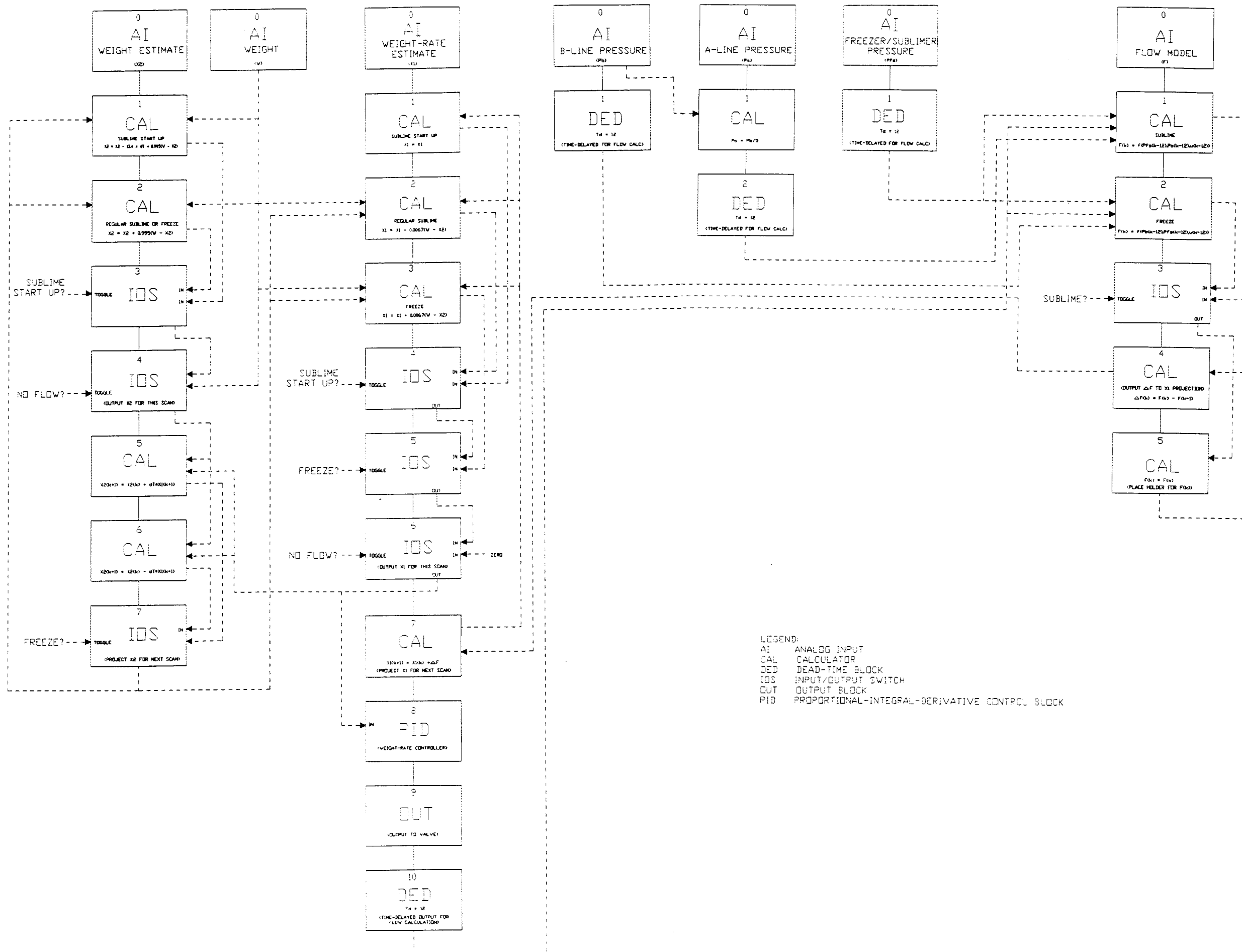


Fig. 3.3. Block diagram of the continuous control strategy for Texas Instruments D/3 implementation.

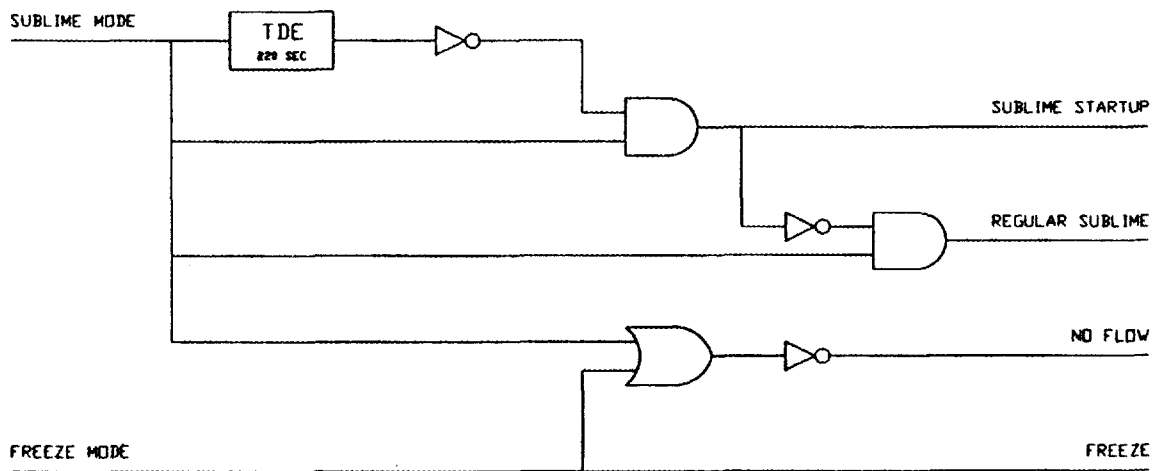


Fig. 3.4. Digital device logic diagram for Texas Instruments D/3 control system implementation.

4. CONTROL STRATEGY

The goal of the Kalman filter is to provide a suitable freeze or sublime rate signal of the freezer/sublimator system that can be used as an input to a controller. This section discusses two types of control strategies to be considered when developing the control strategy. The first makes use of the flow model that was developed in Sect. 2, and the second is a conventional control strategy.

4.1 PROCESS MODEL-BASED CONTROL STRATEGY

An existing method of nonlinear control, process model-based control,⁷ could be used with the flow equation already developed. An explanation of this method follows.

The characterized flow of the prototype freezer/sublimator system as a function of upstream and downstream pressure and valve output is shown by

$$F = \frac{NP_1\sqrt{X}}{\sqrt{1 + \alpha R_v^{2(1-u)}}} \quad (4.1)$$

But what if the equation is solved for u ? This equation would give a steady-state valve output as a function of flow set point as well as upstream and downstream pressure as

$$u = \frac{-\ln(R_v^2 \alpha) + \ln \left[\frac{N^2 P_1 (P_1 - P_2)}{F_{sp}^2} - 1 \right]}{-2 \ln R_v}, \quad (4.2)$$

where F_{sp} is the flow set point.

Figures 4.1, 4.2, and 4.3 show what the behavior of the valve output signal should be relative to the flow set point, upstream pressure, and downstream pressure respectively.

Of course, the calculation block shown in Eq. (4.2) will not perfectly remove biases and other modeling errors; therefore, the loop should be closed with a control block added. But the control block could feed into the calculation block in such a way that the calculation block could linearize the output and adjust it for varying process conditions. Instead of acting on the raw flow set point F_{sp} , the calculation block could act on the controller output U^* . Input ranges to the block would have to be checked to ensure that no divisions by zero or memory overloads occurred in the calculation block.

A block diagram of the proposed scheme along with the Kalman filter is shown in Fig. 4.4.

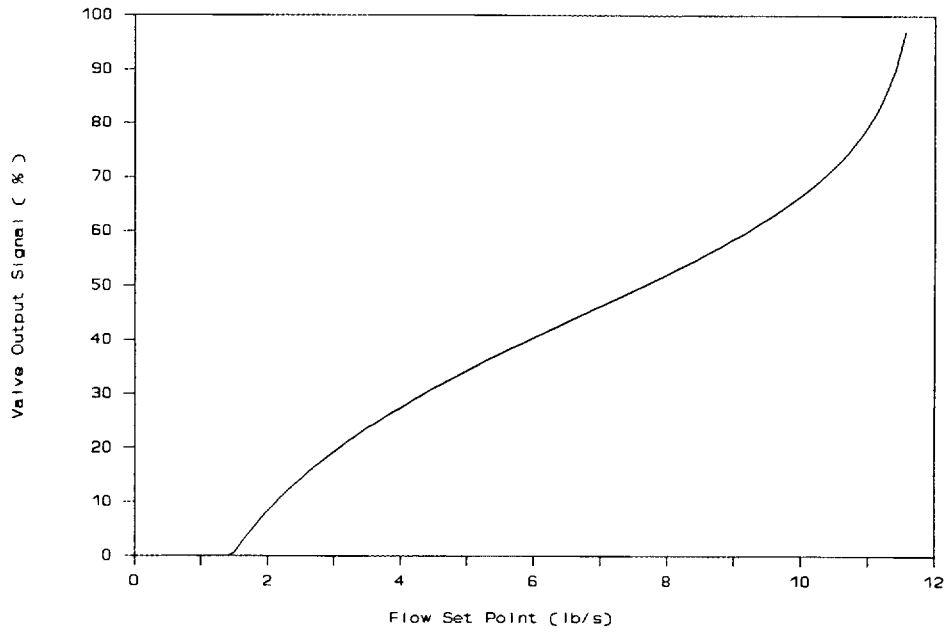


Fig. 4.1. Valve output characterization relative to flow set point with $P_1 = 9$ and $P_2 = 3$.

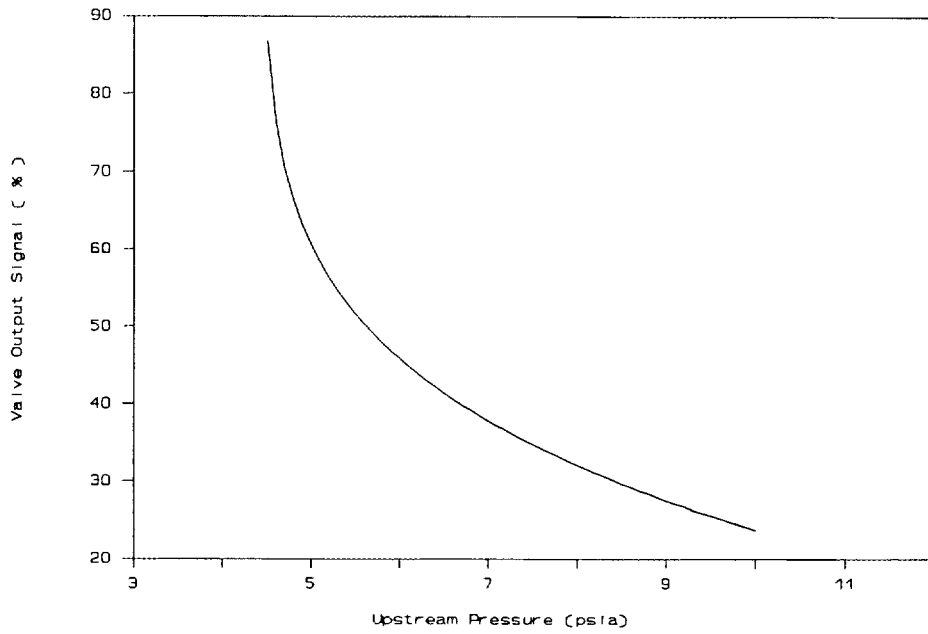


Fig. 4.2. Valve output characterization relative to upstream pressure with $F_{\text{sp}} = 4$ and $P_2 = 3$.

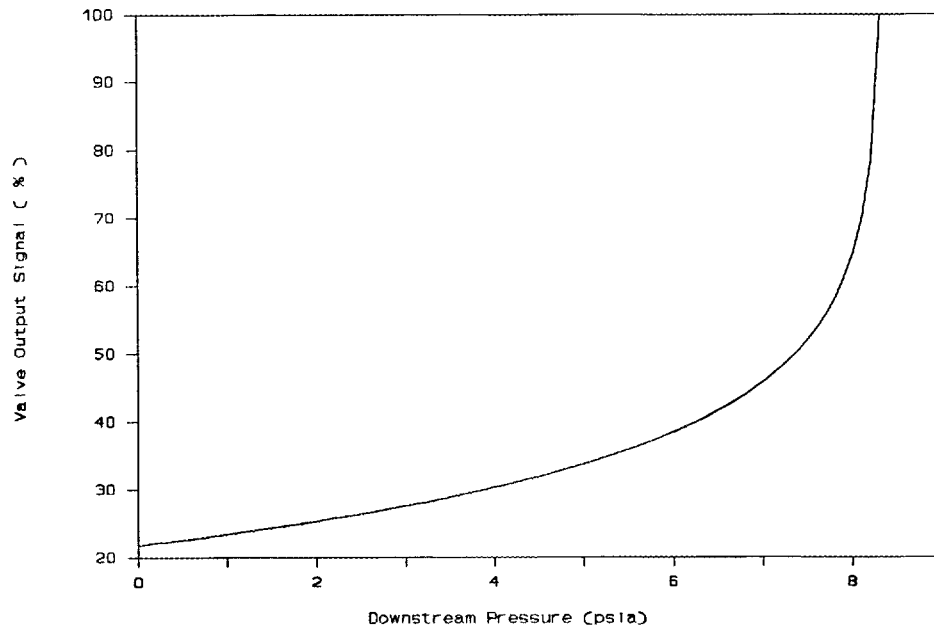


Fig. 4.3. Valve output characterization relative to downstream pressure with $F_p = 4$ and $P_2 = 3$.

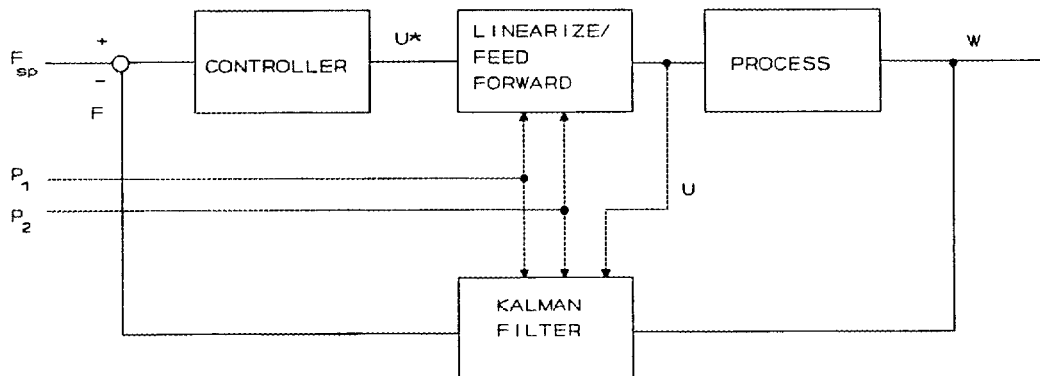


Fig. 4.4. Schematic of nonlinear control strategy using Kalman filter.

4.2 CONVENTIONAL LINEAR CONTROL STRATEGY

Flow is typically one of the fastest responding process variables in industrial manufacturing facilities. Ideally, a control loop should be linearized to capitalize fully on linear feedback control strategies. However, when the time constants involved are small, it does not take long to recover from the effects of controlling a nonlinear system with linear feedback control.

A conventional linear control strategy for the freezer/sublimator system would entail using the Kalman-filtered flow rate as the process variable input to a standard proportional-integral-derivative controller. No linearization would be involved.

5. CONCLUSIONS AND RECOMMENDATIONS

Unless the characteristics of the freezer/sublimator system are found to change drastically with time, we recommend the use of a steady-state Kalman filter to estimate freeze and sublime rates of the freezer/sublimator systems. This strategy is simpler than continuously updating the Kalman gain factors, but preliminary testing indicates that it works for a fairly broad range of test cases. The steady-state Kalman gains can be used for both freeze and sublime modes.

No benefits are foreseen in using a nonlinear control strategy or any other characterization or compensation of the controlled variable. Use of these techniques would only complicate the control system. We recommend the use of conventional linear control strategy.

Because the analysis in this report represents only off-line analysis of actual plant data, we highly recommend that the algorithms be tested on-line with the prototype freezer/sublimator system before using them in the design of the remainder of the control system.

The premise of this report is that using a flow meter to measure flow of UF_6 into and out of the freezer/sublimator vessel is not feasible, because of high costs associated with installation of a meter on several parallel freezer/sublimator systems or because it is simply not practical to install a flow meter in the line for physical or mechanical reasons. If these premises are not true, installation of a flow meter should be addressed.

6. REFERENCES

1. D. T. Camp and J. Wassick, "State Estimation: A Better Way to Get Flow Rates from Weight Measurements," Tutorial/Colloquium on State Estimation in the Chemical Industry, Lehigh University, Bethlehem, Pa., Dec. 15, 1988.
2. P. A. Tapp, et al., "A Process Simulator/Trainer for the Process Inventory Control System 20-MW Freezer/Sublimator," ORNL/TM-11772, Oak Ridge National Laboratory, Oak Ridge, Tenn., May 1991.
3. Instrument Society of America, "Flow Equations for Sizing Control Valves," Standard S75.01, Research Triangle Park, N. C., 1985.
4. Brian Roffel and John E. Rijnsdorp, *Process Dynamics, Control and Protection*, Ann Arbor Science, 1982.
5. Arthur Gelb, ed., *Applied Optimal Estimation*, MIT Press, Cambridge, Mass., 1974.
6. R. G. Brown, *Random Signal Analysis and Kalman Filtering*, Wiley, New York, 1983.
7. James B. Riggs and R. Russell Rhinehart, "Nonlinear Process-Model Based Control," Instrument Society of America Conference, Philadelphia, Pa., October 1989.

Appendix A

**FREEZE AND SUBLIME DATA, WEIGHT-RATE AND WEIGHT COMPARISONS,
AND KALMAN FILTER AND CONTROL ALGORITHM PSEUDOCODE**

Freeze Data

Table A.1. 1106C data

| U, % | F/P ₁ | X _{low} | X _{high} | F/(P ₁ √X) |
|-------|------------------|------------------|-------------------|-----------------------|
| 5.60 | 0.142 | 0.43 | 0.62 | 0.22 |
| 15.95 | 0.213 | 0.38 | 0.42 | 0.34 |
| 36.4 | 0.381 | 0.26 | 0.38 | 0.73 |
| 55.9 | 0.511 | 0.18 | 0.25 | 1.17 |
| 76.2 | 0.539 | 0.15 | 0.18 | 1.37 |
| 96.6 | 0.556 | 0.14 | 0.15 | 1.48 |
| 16.0 | 0.232 | 0.35 | 0.40 | 0.38 |
| 36.2 | 0.397 | 0.20 | 0.33 | 0.83 |
| 56.5 | 0.446 | 0.13 | 0.18 | 1.18 |

Table A.2. 1103C data

| U, % | F/P ₁ | X _{low} | X _{high} | F/(P ₁ √X) |
|------|------------------|------------------|-------------------|-----------------------|
| 5.62 | 0.143 | 0.32 | 0.55 | 0.23 |
| 16.0 | 0.192 | 0.26 | 0.30 | 0.37 |
| 37.1 | 0.330 | 0.16 | 0.26 | 0.81 |
| 57.2 | 0.388 | 0.10 | 0.16 | 1.14 |

Table A.3. 1126A data

| U, % | F/P ₁ | X _{low} | X _{high} | F/(P ₁ √X) |
|------|------------------|------------------|-------------------|-----------------------|
| 36.2 | 0.447 | 0.33 | 0.36 | 0.82 |

Table A.4. 1110A data

| U, % | F/P ₁ | X _{low} | X _{high} | F/(P ₁ √X) |
|-------|------------------|------------------|-------------------|-----------------------|
| 15.93 | 0.232 | 0.34 | 0.40 | 0.38 |

Sublime Data

Table A.5. 1108B data

| U, % | F/P ₁ | X _{low} | X _{high} | F/(P ₁ √X) |
|-------|------------------|------------------|-------------------|-----------------------|
| 15.72 | 0.246 | 0.67 | 0.72 | 0.294 |
| 36.0 | 0.593 | 0.67 | 0.72 | 0.714 |
| 56.5 | 0.838 | 0.55 | 0.67 | 1.086 |
| 77.0 | 1.03 | 0.46 | 0.55 | 1.459 |
| 105.8 | 1.11 | 0.44 | 0.46 | 1.661 |

Table A.6. 1103E data

| U, % | F/P ₁ | X _{low} | X _{high} | F/(P ₁ √X) |
|------|------------------|------------------|-------------------|-----------------------|
| 15.7 | 0.254 | 0.73 | 0.76 | 0.294 |
| 36.2 | 0.582 | 0.67 | 0.76 | 0.693 |
| 56.9 | 0.837 | 0.54 | 0.67 | 1.095 |
| 77.2 | 1.06 | 0.40 | 0.54 | 1.569 |
| 98.7 | 1.13 | 0.21 | 0.40 | 1.84 |
| 5.29 | 0.248 | 0.66 | 0.71 | 0.300 |

Table A.7. 1105C data

| U, % | F/P ₁ | X _{low} | X _{high} | F/(P ₁ √X) |
|------|------------------|------------------|-------------------|-----------------------|
| 16.8 | 0.277 | 0.76 | 0.80 | 0.313 |
| 36.6 | 0.601 | 0.75 | 0.80 | 0.687 |
| 5.04 | 0.286 | 0.73 | 0.76 | 0.332 |

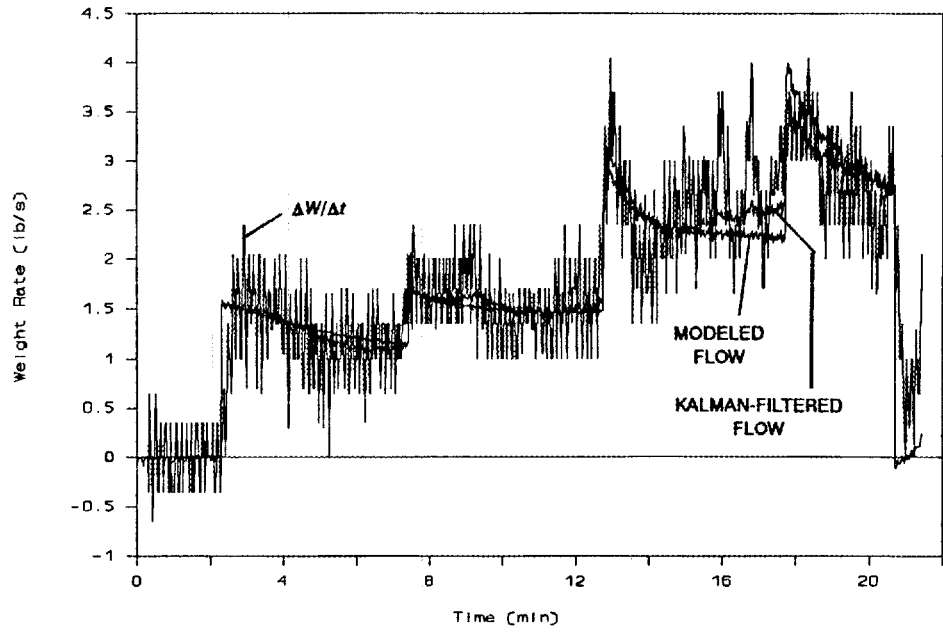


Fig. A.1. Test 1103C weight-rate comparison.

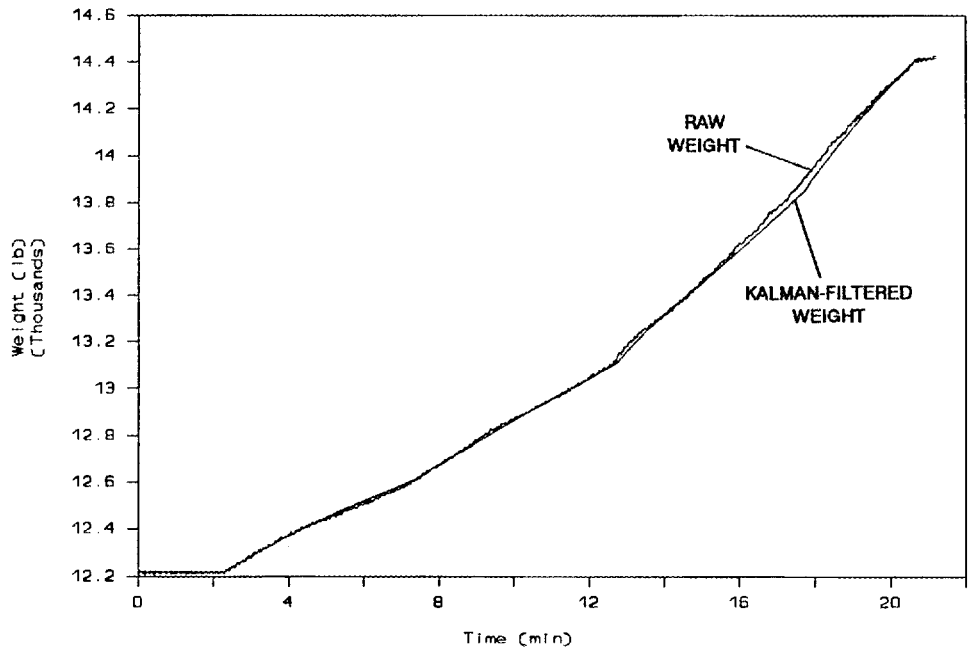


Fig. A.2. Test 1103C weight comparison.

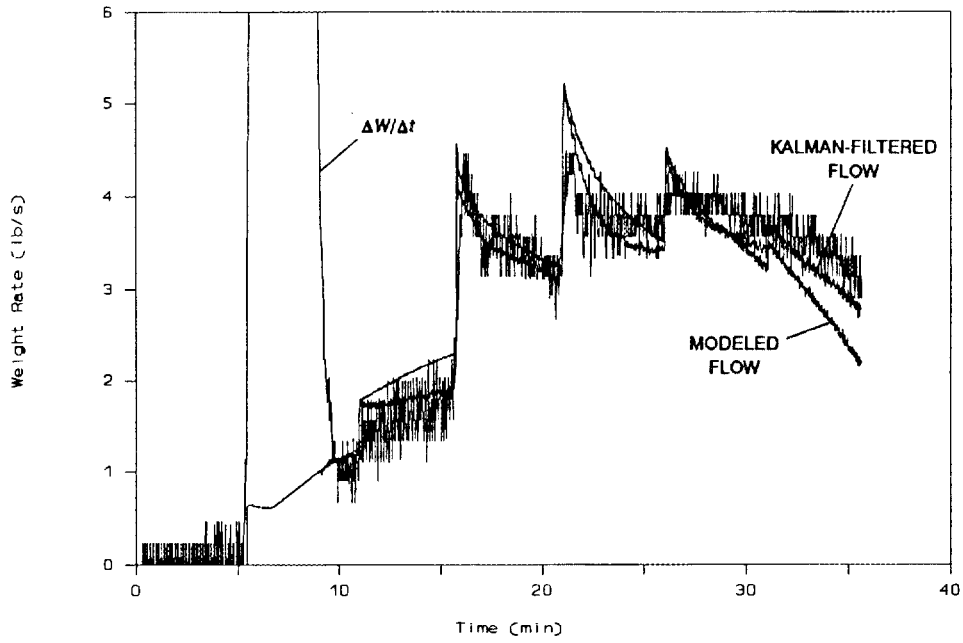


Fig. A.3. Test 1103E weight-rate comparison.

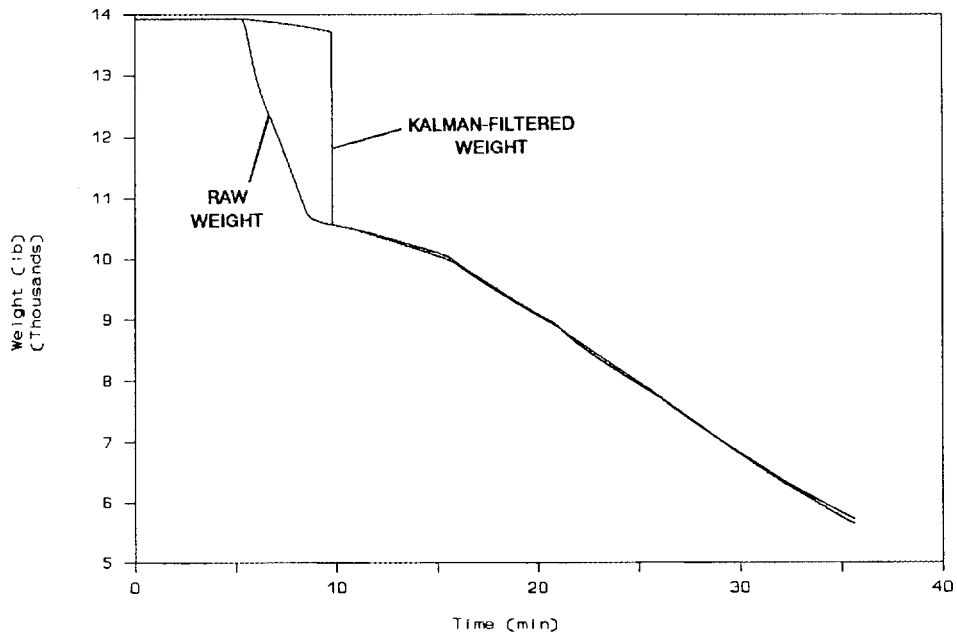


Fig. A.4. Test 1103E weight comparison.

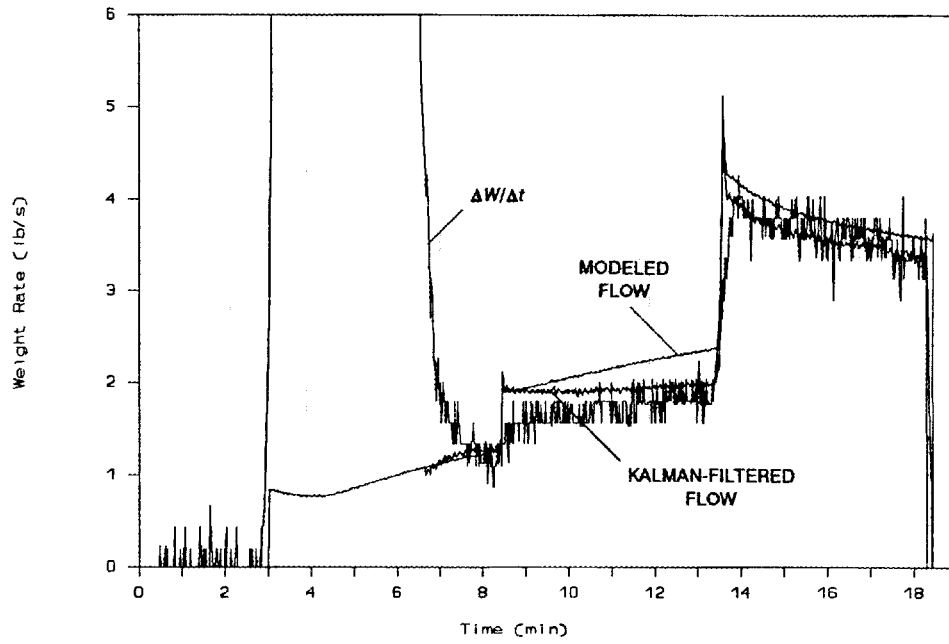


Fig. A.5. Test 1105C weight-rate comparison.

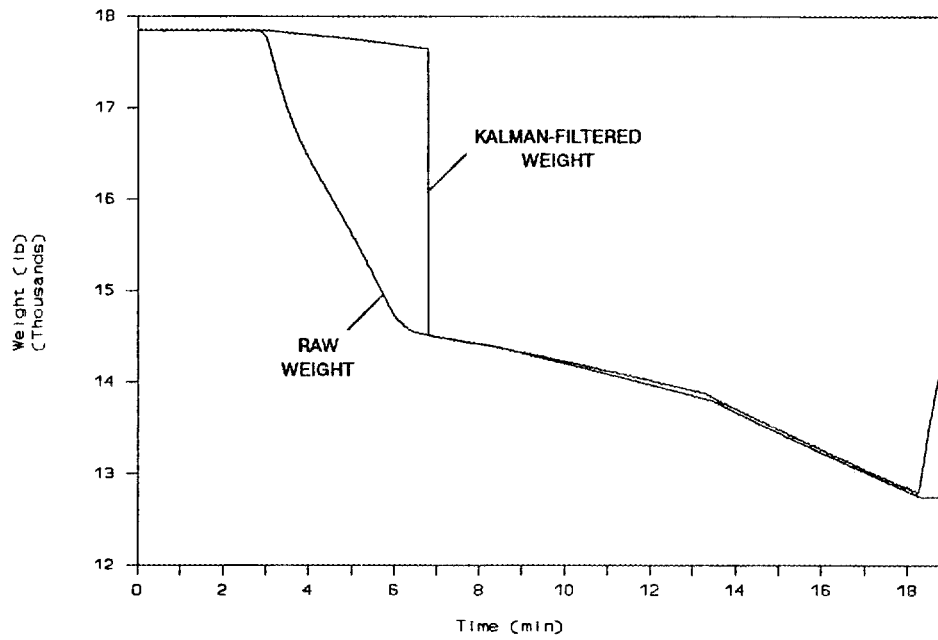


Fig. A.6. Test 1105C weight comparison.

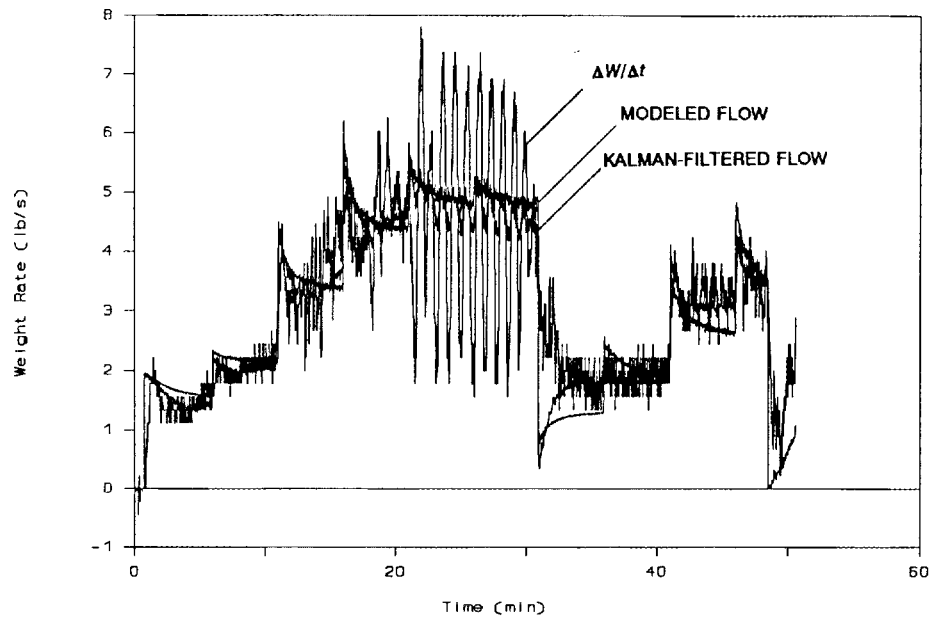


Fig. A.7. Test 1106C weight-rate comparison.

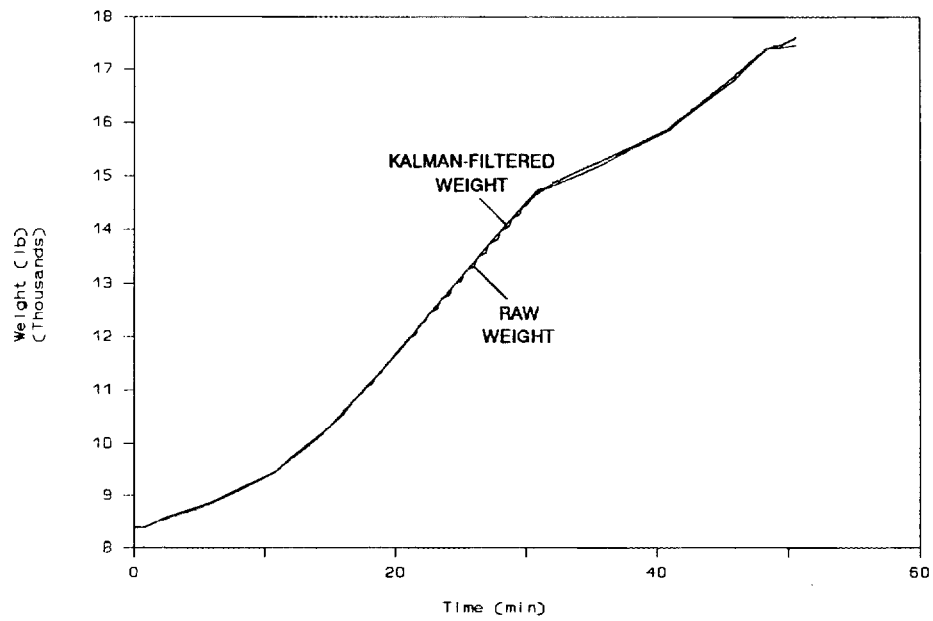


Fig. A.8. Test 1106C weight comparison.

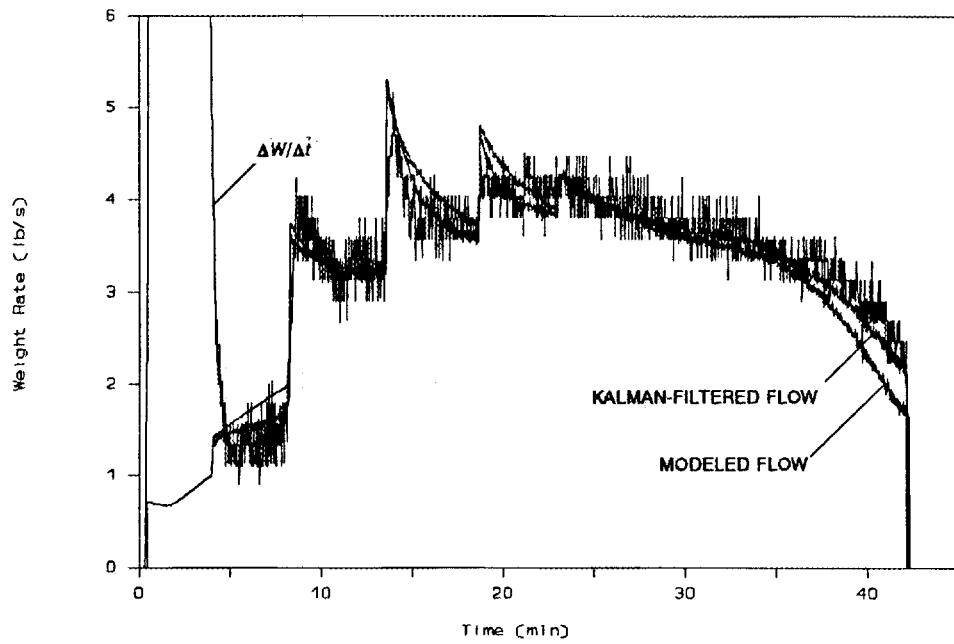


Fig. A.9. Test 1108B weight-rate comparison.

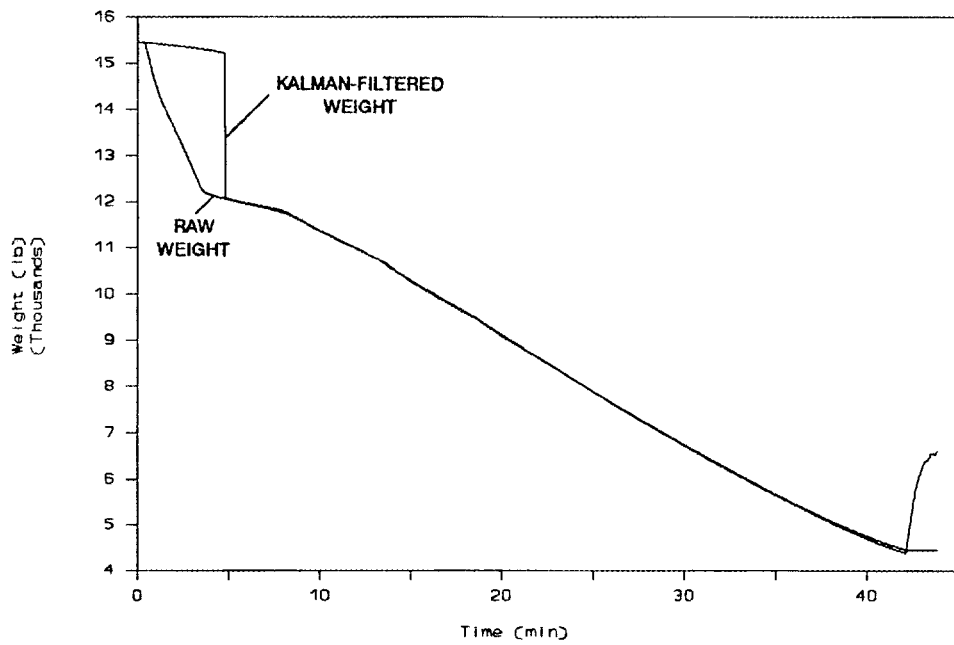


Fig. A.10. Test 1108B weight comparison.

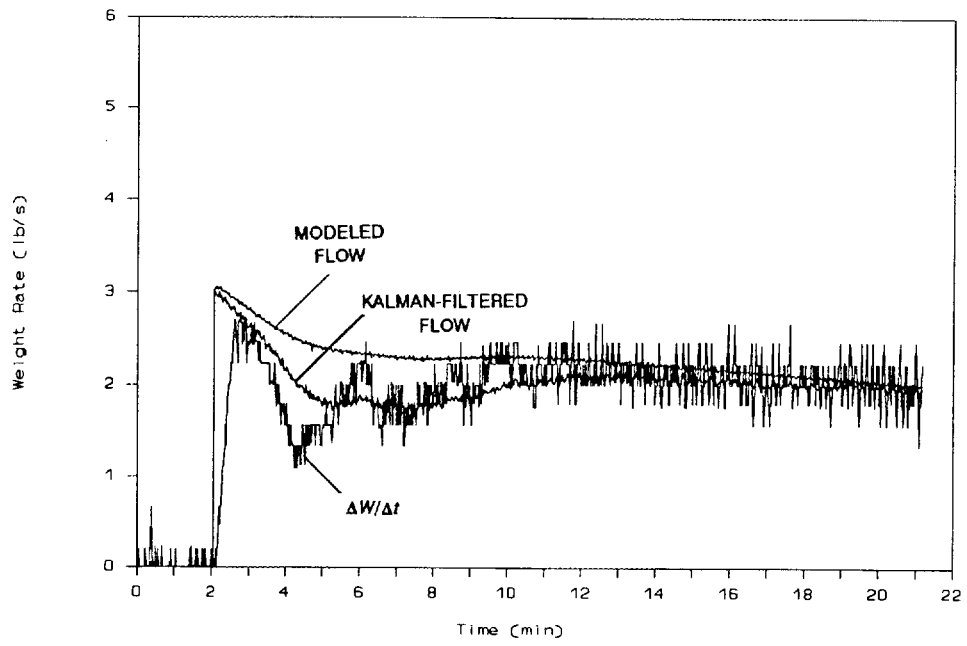


Fig. A.11. Test 1110A weight-rate comparison.

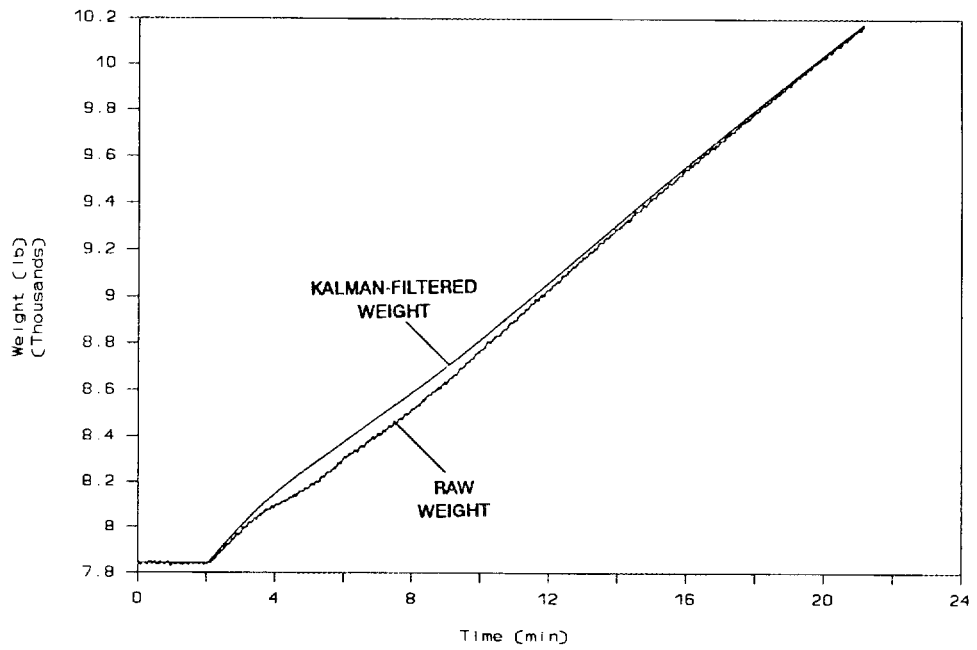


Fig. A.12. Test 1110A weight comparison.

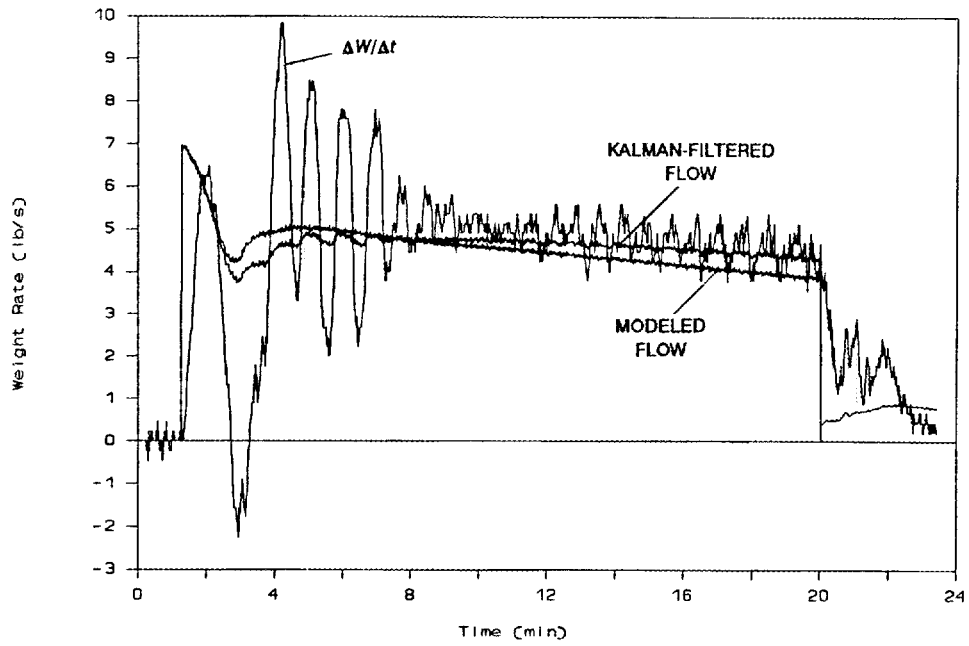


Fig. A.13. Test 1126A weight-rate comparison.

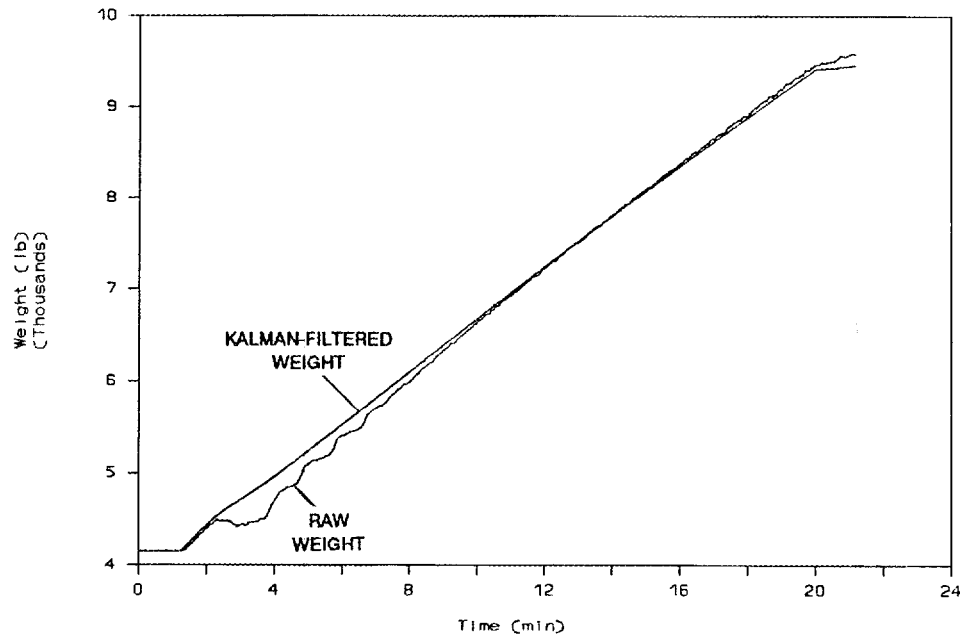


Fig. A.14. Test 1126A weight comparison.

'Kalman Filter and Control Algorithm Pseudocode

DIM S(-12 TO 0), P1(-12 TO 0), P2(-12 TO 0), PY301(-12 TO 0), E(-1 TO 0), F(0 TO 1)

dT = 1 'scan period in seconds
Kc = 1.5 'controller proportional gain used in simulations
Ki = 0.4 'controller reset rate used in simulations

'Set initial conditions of estimates

X1 = 0 'flow estimate
X2 = 0 'weight estimate

'Begin looping

DO

 'Reset variables in FIFO arrays

 FOR i = -12 to -1

 S(i) = S(i+1)

 P1(i) = P1(i+1)

 P2(i) = P2(i+1)

 PY301(i) = PY301(i+1)

 NEXT i

 'Read new variables for this scan

 READ S, UPRES, PT306, W

 S(0) = S

 PY301(0) = PY301

 'Set new values of array variables

 IF S = 53 THEN

 'F/S is in sublime mode

 P1(0) = PT306

 P2(0) = UPRES/5

 ELSEIF S = 66 THEN

 'F/S is in freeze mode

 P1(0) = UPRES

 P2(0) = PT306

 ENDIF

 'This section of code checks to see if the F/S has just been switched to sublime mode.

 'If it has, a flag is set for 220 s. During this time, the F/S weight input is ignored,

 'and the controller acts on the modeled flow only.

 IF S(-11) <> 53 THEN

 SublimeStartup% = false%

 Timer = 0

 ENDIF

 IF S(-11) = 53 AND S(-12) <> 53 THEN SublimeStartup% = true%

 IF SublimeStartup% THEN

 Timer = Timer + 1

 IF Timer > 220 THEN

 SublimeStartup = false%

 Timer = 0

 ENDIF

 ENDIF

```

Update estimates
IF SublimeStartup% THEN
    X1 = X1
    X2 = X2 - 13.4 * dT + 0.995 * (W - X2)
ELSEIF S(-11) = 66 THEN
    X1 = X1 + 0.0067 * (W - X2)
    X2 = X2 + 0.995 * (W - X2)
ELSEIF S(-11) = 53 THEN
    X1 = X1 - 0.0067 * (W - X2)
    X2 = X2 + 0.995 * (W - X2)
ELSE
    X1 = 0
    X2 = W
ENDIF

```

'ignore weight input during sublime startup
'freon transfers around 13.4 lb/s

'freeze mode weight rate
'freeze mode weight

'sublime mode weight rate
'sublime mode weight

'weight rate = 0 except in freeze or sublime mode
'use raw weight input

'Set old and new error terms

E(-1) = E(0)
E(0) = SP - X1

'Control Algorithm (PI mode--no derivative)

PY301 = PY301 + Kc * (E(0) - E(-1)) + Ki * dT * E(0)

'Limit control output between 0 and 100%

IF PY301 > 100 THEN PY301 = 100
IF PY301 < 0 THEN PY301 = 0

'Calculate modeled flow

F(0) = F(1)

IF S(-11) = 53 OR S(-11) = 66 THEN

F(1) = 1.6 * P1(-11) * SQR((P1(-11) - P2(-11)) / P1(-11)) / SQR(1 + 0.029 * 47 ^ (2 * (1 - (PY301(-11) / 100))))

ELSE

F(1) = 0 'set modeled flow to zero if not in freeze or sublime mode

ENDIF

'Project new estimate for next scan

X1 = X1 + F(1) - F(0)

'weight rate

IF S = 66 THEN X2 = X2 + dT * X1

'weight (increases in freeze mode)

IF S = 53 THEN X2 = X2 - dT * X1

'weight (decreases in sublime mode)

LOOP

END

Variable Definitions

Kc = controller proportional gain
Ki = controller integral term (resets/s)
PT306 = freezer/sublimer pressure (psia)
PY301 = controller output signal to valve (%)
S = freezer/sublimer status (53 = sublime, 66 = freeze)
SP = controller set point (lb/s)
Timer = freon weight shift timer at beginning of sublime mode
UPRES = upstream stage 4 pressure (psia)
W = measured weight (lb)
X1 = estimated weight rate (lb/s)
X2 = estimated weight (lb)

Arrays

Arrays are used to store past values of key variables to enable calculating flow with deadtime and to track past values of other variables.

E() = controller error term array

F() = flow model array (lb/s)

P1() = general upstream pressure used for both freeze and sublime modes (= UPRES in freeze mode, = PT306 in sublime mode)

P2() = general downstream pressure used for both freeze and sublime modes (= PT306 in freeze mode, = UPRES/5 in sublime mode)

S() = freezer/sublimer status array

PY301() = valve output array

INTERNAL DISTRIBUTION

- | | |
|---------------------|--------------------------------------|
| 1. H. R. Brashear | 30. J. N. Sumner |
| 2. J. N. Davis | 31. R. E. Uhrig |
| 3-5. W. R. Devan | 32. B. G. Warriner |
| 6. B. C. Duggins | 33. T. W. Wilder |
| 7. B. G. Eads | 34. B. Chexal, Advisor |
| 8. D. N. Fry | 35. V. Radeka, Advisor |
| 9. J. M. Googe | 36. R. M. Taylor, Advisor |
| 10. S. S. Gould | 37. Applied Technology Library |
| 11. D. E. Gray | 38-39. ORNL Central Research Library |
| 12. J. E. Hardy | 40. PORTS Library Services |
| 13. D. M. Herricks | 41. PGDP Records |
| 14. D. W. McDonald | 42. PGDP Plant Library |
| 15. C. S. Meadors | 43. Y-12 Technical Reference Section |
| 16. D. R. Miller | 44-45. Laboratory Records |
| 17. J. T. Patton | 46. Laboratory Records-Record Copy |
| 18. R. D. Raney | 47. ORNL Patent Section |
| 19-28. F. R. Ruppel | 48. I&C Division Publications Office |
| 29. J. O. Stiegler | |

EXTERNAL DISTRIBUTION

49. Assistant Manager for Energy Research and Development, DOE-OR,
P. O. Box 2001, Oak Ridge, TN 37831-8600
- 50-173. Given distribution as shown in DOE/OSTI-4500 under Category UC-506,
Instruments, Engineering, and Equipment

